UNIVERSITY OF TARTU

Faculty of Science and Technology

Institute of Chemistry

ISOTOPIC STABILITY OF MASS REFERENCE MATERIALS AND POSSIBLE USE AS ISOTOPIC REFERENCE MATERIALS

Margarita Esmeralda Gonzales Ferraz

Master's Thesis

(30 ECTS)

Applied Measurement Science

Supervisors:

Kalle Kirsimäe

Holar Sepp

Department of Geology, University of Tartu

Tartu-Estonia

2020

List of abbreviations

CF-IRMS Continuous flow Isotope Ratio mass spectrometer

DOC Dissolved Organic Carbonate

EA Elemental Analyser

GC Gas Chromatography

IAEA International Atomic Energy Agency

NIST National Institute of Standards and Technology

POC Particulate Organic Carbon

SLAP Standard Light Antarctic Precipitation (now replaced by SLAP2)

SMOW Standard Mean Ocean Water

TC/EA-IRMS Thermal Conversion /Elemental analyser Isotope Ratio Mass Spectrometry

VPDB Vienna Peedee Belemnite from the Cretaceous formation in South Carolina

VSMOW Vienna Standard Mean Ocean Water.

Table of Contents

1. INTRODUCTION

Stable isotope research has developed to the point where thousands of isotope ratio mass spectrometers are in operation in laboratories all over the world. Stable isotope measurements have an extremely wide range of applications and are being made to resolve problems in many diverse fields including geochemistry, climatology, hydrology, plant physiology, ecology, archaeology, meteorology, meteoritics, palaeobiology, bacteriology and the origin of life [1].

Natural Isotope variation or fractionation depends on thermodynamic equilibria and kinetic processes affecting the individual isotope. In both cases, fractionation is a function of slight variation in the physical and chemical properties of the isotopes and its proportional to differences in their masses [2].

The primary standard accepted for relative nitrogen (N) isotope-ratio measurements is atmospheric nitrogen (N_2) gas, which is widespread and homogeneous and, by convention, has a δ^{15}N value of 0‰ [3]. The primary standard for carbon (C) isotope-ratio measurements since 1993 should be reported relative to VPDB (Vienna PDB) having a δ^{13}C value of 0‰ [4]. These standards are available to investigators for use in calibrating the working standards with individual mass spectrometer laboratories.

Isotope ratio analysis involves precise measurement, usually by mass spectrometry, of the more abundant light isotope relative to the less abundant heavy isotope [5].

The old laborious extraction techniques for a stable isotope analysis were developed by analytical chemists who were very concerned about reproducible, quantitative chemical reactions.

The application of multicollector-ICP-mass spectrometry now enables investigations of stable isotope compositions with adequate precisions for a wide range of transition and heavy elements that could not be measured before [6].

In any isotopic analysis, very precise and analytical techniques are required. Isotopic composition is measured by determining the ratios of the two stables isotopes present in the sample. It has been found that measuring the absolute isotopic composition is not as reliable and or convenient as measuring isotopic differences between a sample and a given standard. This is because while obtaining high precision in absolute isotopic composition of a sample is not difficult over short term, but it is difficult over long term. In contrast, analysis based on the measurement of the differences between a defined standard and sample provide high precision and repeatability over short and long term periods [2]. Because of instrumental requirements,

carbon and nitrogen must be converted to CO_2 and N_2 for stable ratio measurements. Most of the error associated with isotopic measurements results from sample preparation [4].

Stable isotope ratio mass-spectrometry laboratory at Department of Geology, Tartu University has been in operation for more than 10 years. While primarily aimed at Carbon and Oxygen isotope composition of carbonate phases via phosphoric acid (H_3PO_4) dissolution method. Then since 2014, the laboratory has been measuring C and N isotope composition of solid organic and inorganic geological, archaeological, and biological materials. In element analyser attached to isotope ratio mass-spectrometer the element composition of the C and N are analysed along with their isotopic compositions using calibration against the known composition of respective reference materials.

1.1. OBJETIVE

The aim of this work was to study and analyse the stability and long-term within laboratory reproducibility of the $\delta^{15}N$ and $\delta^{13}C$ composition of the different standard reference materials - for the Acetanilide, Aspartic Acid and Nicotinamide - routinely used for the calibration of C and N abundance (mass %) in data collected with the Elemental analyser attached with the Continuous Flow-Isotope Ratio Mass Spectrometer (CF-IRMS) from the geology department of University of Tartu. This study estimates the possibility to use the Elemental analyser reference materials as secondary isotope standards.

2. LITERATURE REVIEW

2.1. STABLE ISOTOPES

Isotopes are atoms of an element that share the same number of protons but a different number of neutrons. In the scientific nomenclature, isotopes are specified in the form ${}^{m}_{n}E$, where "m" indicates the mass number (the sum of protons and neutrons in the nucleus) and "n" refers to the atomic number of an element "E" [2].

Stable isotopes are those isotopes of an element that are stable and do not decay through radioactive processes over time [4]. Although they do not emit radiation, their unique properties enable them to be used in a broad variety of applications, including water, soil management, environmental studies, nutrition assessment studies and forensics. Eighty out of the first 82 elements in the periodic table have stable isotopes. Stable isotopes can be used by measuring their amounts and proportions in samples. Naturally occurring stable isotopes of water and other substances are used to trace the origin, history, sources and interactions in water, C and N cycles. Variations in stable isotopes ratios in nature are small then can be used as tracers. For this purpose, they are separated using highly sophisticated techniques, such as mass spectrometry [7].

Classical stable isotope geochemistry concerns, mostly for variations in the stable isotope ratios of only five elements: Carbon , Nitrogen , Hydrogen , Oxygen, and Sulphur [1]. Most elements consist of more than one stable isotope [4].

Of the five nitrogen isotopes, ${}^{13}_{7}N$, ${}^{14}_{7}N$, ${}^{15}_{7}N$, ${}^{16}_{7}N$ and ${}^{17}_{7}N$, three are highly unstable with half-lives for ${}^{13}_{7}N$, ${}^{16}_{7}N$, ${}^{17}_{7}N$ of 10 minutes, seven seconds, and four seconds. The only two stable nitrogen isotopes are ${}^{14}_{7}N$ (99.635%) and ${}^{15}_{7}N$ (0.365%) [8].

The element Carbon exist as two stable isotopes ${}^{12}_{6}C$ (98.89 %) (reference mass for atomic weight scale) ${}^{13}_{6}C$ (1.11 %) [4].

2.2. ISOTOPIC FRACTIONATION PROCESS

The partitioning of isotopes between two phases of the same substance with different isotope ratios is called "isotope fractionation". Fractionation during equilibrium (reversible) or disequilibrium (unidirectional) process results because atomic masses and bond strengths differ for different isotopes [5]. There are two different fractionation processes:

A. **Equilibrium isotope distribution (Isotope exchange reactions):** They are mainly driven by changes in the internal energy of a molecule like vibrations of the atoms within a molecule.

Isotopic equilibrium exchange reactions involve redistribution of isotopes of an element among phases or chemical species. At isotopic equilibrium, the forward and backward reactions rates of the lighter isotopic species are equal to those of the heavier isotopic species [5]. For example during equilibrium, volatilization, or dissolution of gases such as CO_2, the heavier isotope tends to concentrate in the aqueous phase because the lighter isotope has a higher vapour pressure [9]. Equilibrium processes take place in close or semiclosed systems [5]. For isotope exchange reactions in geochemistry, the equilibrium constant K is often replaced by the fractionation factor α. The fractionation factor is defined as the ratio of the numbers of any two isotopes in one chemical compound A divided by the corresponding ratio for another chemical compound B (Eq.1):

$$\alpha A\text{-}B = R_A/R_B \qquad \text{(Eq.1)}$$

The equilibrium fractionation factor $\propto_{eq.}$ is related to the equilibrium constant K for two substances as shown in (Eq.2), where n is the number of atoms exchanged in the reaction [10].

$$\propto_{eq.} = k^{\frac{1}{n}} \qquad \text{(Eq.2)}$$

It has become common practice in recent years to replace the fractionation factor α by the ε value (or isotope enrichment factor) which is defined as (Eq.3).

$$\varepsilon = \alpha - 1 \qquad \text{(Eq.3)}$$

because ε × 1000 approximates the fractionation in parts per thousand, like the δ-value [11].

B. **Kinetic fractionation processes:** which depend primarily on differences in reaction rates of isotopic molecules. Are common in nature and in the laboratory [10]. Kinetic fractionation processes are also associated with incomplete and unidirectional processes like evaporation, dissociation reactions, biologically mediated reactions and diffusion [12]. Kinetic fractionation can result in non-equilibrium system in which reactions rates are mass dependent. As a rule, the lighter isotope reacts faster than heavier isotope. Isotopically light molecules can diffuse out of a system and leave the reservoir enriched in the heavy isotope [5][10]. In the case of evaporation or sublimation the system is open, and the volatile, isotopically lighter product can escape, which leads to wide variations in delta values of the

product and residual reactant [13]. During evaporation, the greater average transitional velocities of lighter molecules allows them to break through the liquid surface preferentially resulting in a isotope fractionation between the liquid and vapor [5].

The degree of isotopic fractionation associated with a reaction is commonly expressed with $\propto$, (Eq.4) which is the ratio of rate constants for molecules containing the different isotopes:

$$\propto = \frac{^{14}K}{^{15}K} \quad \text{(Eq.4)}$$

where ^{14}k and ^{15}k are the rate constants for molecules containing the light and heavy isotopes, respectively [11].

Molecules containing the heavy isotopes are more stable and have higher dissociation energies than those containing the light isotope. Kinetic effects are rare in high temperature processes occurring on Earth [10].

2.2.1. ISOTOPIC FRACTIONATION PROCESSES OF NITROGEN

2.2.1.1. NITROGEN

No other essential element for life takes as many forms in soil as N, and transformations among these forms are mostly mediated by microbes. The most important N forms in the biosphere are N_2; dissolved nitrate (NO_3^-), nitrite ($NO_{2)}^-$, ammonium ($NH_{4)}^+$), and organic-N; mineral fixed NH_4^+, and organic N compounds [5][8] .

In nature, N has nine different oxidation states (Table 1), as different types of chemical species, and redox reactions between these species are key components for the N cycle [14].

Table 1. Main forms of Nitrogen in soil and their oxidation states [14].

Name	**Chemical Formula**	**Oxidation State**
Nitrate	NO_3^-	+5
Nitrogen dioxide (g)	NO_2	+4
Nitrite	NO_2^-	+3
Nitric oxide (g)	NO	+2
Nitrous oxide (g)	N_2O	+1
Dinitrogen (g)	N_2	0
Ammonia(g)	NH_3	-3
Ammonium	NH_4^+	-3
Organic N	R_{NH3}	-3
Gases (g) occur both free in the soil atmosphere as well in dissolved in soil water		

N is a trace phase in rocks and the major component of air. ^{15}N is the less abundant isotope consequently is more practical to measure the difference or ratio of two isotopes instead of the absolute quantity of each. The ratio of $^{15}N/^{14}N$ in the air is 272±0.3‰ and this ratio is constant

and allow air N to be used as standard. Solid reference samples are used from NIST and IAEA [1].

Isotopic compositions are expressed in terms of "delta" (δ) values which are given in parts per thousand or per mil (‰). The δ^{15}N-value in the sample is then calculated by the following equation (Eq. 5) [12][15]:

$$\delta^{15}\mathrm{N}(‰ \text{ vs Air}) = \frac{\mathrm{Rsample}}{\mathrm{RStandard}} - 1 * 1000 = \left(\frac{\frac{^{15}\mathrm{N}}{^{14}\mathrm{N}_{\mathrm{Sample}}}}{\frac{^{15}\mathrm{N}}{^{14}\mathrm{N}_{\mathrm{air}}}} - 1 \right) * 1000 \qquad \text{(Eq.5)}$$

where R_{sample}, $R_{standard}$ is a ratio of heavy isotope to light isotope, in the examined sample and the standard one, respectively. A positive δ value means enrichment, and negative δ depletion of the sample in the heavy isotope of a given element. A suitable value in isotopic studies is isotopic fractionation, εp/s, expressed in Eq. 6:

$$\frac{\varepsilon \mathrm{p}}{\mathrm{s}(‰)} = \left(\frac{\delta^{15}\mathrm{Nproduct} - \delta^{15}\mathrm{Nsubstrate}}{\delta^{15}\mathrm{Nsubstrate} * 1000} \right) * 1000 \approx \delta^{15}\mathrm{Nproduct} - \delta^{15}\mathrm{Nsubstrate} \qquad \text{(Eq.6)}$$

If $\varepsilon_{\rho/s} > 0$, then the product is enriched in ^{15}N, if $\varepsilon_{\rho/s} < 0$ – depleted; between factors $\varepsilon_{\rho/s}$ and $\varepsilon_{s/\rho}$ is relationship: $\varepsilon_{\rho/s} = -\varepsilon_{s/\rho,}$ where s and p refer to substrate and product, respectively. This value is useful to describe quantitative changes in biogeochemical processes and theoretical modelling of N cycle [11][15].

N isotopic fractionation occurs during the transformation from the reactant to the product. The most significant fractionation effects in the low temperature N system are going to be kinetic [1].

2.2.1.2. BIOLOGICAL NITROGEN ISOTOPIC FRACTIONATION

The size of the largest N reservoir, the Earth atmosphere, and its long residence time of approximately 17 million years suggest that the global N-cycle was likely to be balanced at geological time scales. After the industrial revolution, human activities, such as mining, fossil fuel burning, land use change, and artificial fertilization, have resulted in perturbations and numerous flux changes of the N-cycle [16].

Today, the Earth's atmosphere is about 78% N, about 21% O_2, and about 1% other gases [17]. N is capable of being transformed biochemically or chemically through several processes summarized as the N-cycle (Figure 1). Photoautotrophic plants, heterotrophic organisms and nitrifying bacteria form the N-cycle [18].

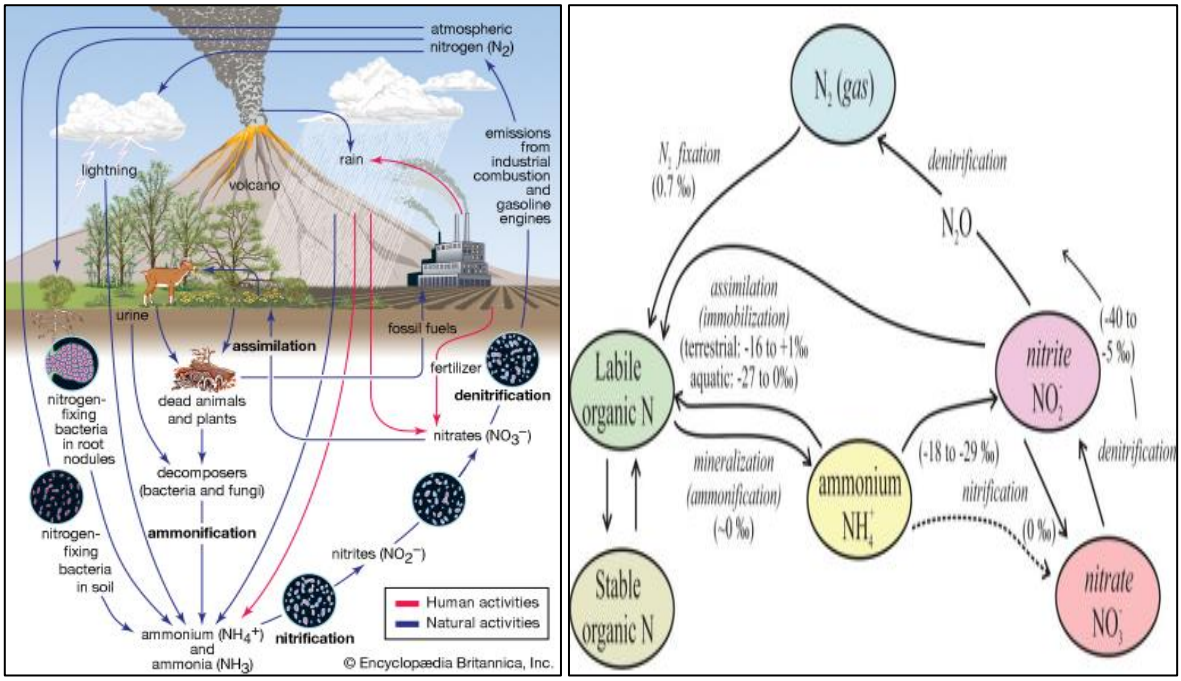

a) b)

Figure 1. a) Nitrogen Cycle b) Simplified diagram of the diagram of nitrogen cycle. Note that nitrification is generally thought of a the conversion of nitrate to N_2 and/or N_2O gas, but that nitrite is an intermediate phase. Numbers is parenthesis indicate average fractionations (δ^{15}Nproduct- δ^{15}N source) associated with each process [1][19].

Mayor biochemical N-cycle processes include:

A. Nitrogen Fixation

Is a conversion of atmospheric N_2 to NH_3 which can be metabolized in cells of living organisms. N_2-fixing bacteria are both aerobic and anaerobic. Two kinds of N-fixing bacteria are recognized.

- **Nitrogen-Fixing Symbiosis:** N-fixing bacteria can transform atmospheric N_2 into fixed N and form symbiotic associations (with groups of plants and some fungi). Comprises the mutualistic Rhizobium (leguminous plants), *Frankia (*dicotyledonous species), certain *Azospirillum* species (cereal grasses) [20].

- **Non-Symbiotic Nitrogen Fixation**: Biological fixation of atmospheric N_2 is catalysed by the nitrogenase enzyme complex and synthetized by limited number of bacteria (*prokaryotes*) [21].

- **N_2 Fixation by lightning:** High temperatures occurring in lightning strikes produce NO in the atmosphere from molecular oxygen (O_2) and N. The NO is oxidized to NO_2 and then to Nitric acid (HNO_3) which is removed by wet and dry deposition thus introducing N into ecosystems [21][22].

N fixation is generally considered as a single process in terms of isotopic fractionation, because $\delta^{15}N$ values are measured on the product plant or bacterium, regardless of the pathway from $N_2(g)$ to organic matter. N isotope fractionation associated with fixation is generally small [1]. Fixation commonly produces organic materials with $\delta^{15}N$ values slightly less than 0 ‰, ranging from -3 to +1‰ [11].

B. Assimilation or Immobilization

Is the process of ingestion by plants of simple inorganic compounds containing N, such as NO_3^-, NO_2^- and NH_4^+. In the presence of a suitable reductase, NO_2^- or NO_3^- ions are reduced to NH_4^+ ions, which are converted to organic matter [15]. There is no appreciable difference between assimilation of NH_4^+, NO_2^-, and NO_3^-. Higher plants show much smaller fractionations, averaging -0.25‰ and assimilation for aquatic plants range between -27 to 0 ‰ [1].

C. Dissimilation

Is the use by bacteria in anaerobic conditions of oxidized N form (NO_3^- or NO_2^-), as an alternative of electrons acceptor to the free oxygen. NO_3^- reduction leads in this case to producing NO_2^- or NH_3. This process is generally referred to as nitrate respiration [15].

D. Mineralization (Ammonification)

Is the decomposition of complex organic compounds containing N into NH_3 or NH_4^+.The mineralization is in soils generally a slowly but continuous ongoing process with a very wide range of conditions especially concerning soil moisture and soil temperature and is still active above 70ºC [15].

The mineral N (N_{min}) is the sum of NH_4^+ and NO_3^- present in the soil solution or as exchangeable ions. Temperature and humidity play an important role. Generally, less water availability and stronger temperature changes decrease mineralization. When drought problems occur, or temperature changes are observed, NO_3^- concentration decreases in favour of increasing accumulation of NH_4^+ [18]. The fractionation associated with breakdown of organic matter to soil ammonium is small 0±1‰ [1].

E. Nitrification

Nitrification is the process of conversion of NH_4^+ to NO_2^- and then to NO_3^-(favourable conditions) [12][23][24].The optimum temperature for nitrification ranges from 30–35°C. Nitrification is also sensitive to soil pH, nitrification is negligible below pH 4.5 [13]. According to Park et.al. [25] the pH optimal for *Nitrosomonas*-Ammonia Oxidizing Bacteria (AOB) lye in

the range of 8.2 ± 0.3 and 7.9±0.4 for *Nitrobacter* -Nitrite Oxidizing Bacteria (NOB), being NOB more sensitive for pH ranges.

Nitrification is a two-steps process carried out by three microbial groups (1) autotrophic ammonia oxidizers, (2) autotrophic nitrite oxidizers and (3) heterotrophic nitrifiers.

The first step: The Ammonia oxidation bacteria-Autotrophic ammonia oxidizers (AOB) to nitrite Included in this group of bacteria are: *Nitrosomonas, Nitrosococuss, Nitrosospira, Nitrosovibria, Nitrosolobus* [14][15].

Nitrosomonas converts NH_4^+ to NO_2^- (Eq.5) and to N_2O in less toxic conditions.

$$2NH_4^+ + 3O_2 \rightarrow 2NO_2^- + 4H^+ + 2H_2O + \text{Energy} \quad \text{(Eq.5)}$$

Since there is production of $2H^+$ per N during nitrification, this may cause acidification in some environments.

The second step: Autotrophic nitrite oxidizers-*Nitrobacter* oxidizes NO_2^- to NO_3^- [1] (Eq.6). Autotrophic nitrifiers can be considered "keystone species" and their disappearance, because of negative impacts by pollutants [21]. Autotrophic nitrifiers are inactivated by many organic compounds, and are poor competitors for NH_4^+ and NO_2^- compared to heterotrophs [23]

$$2NO_2^- + O_2 \rightarrow 2NO_3^- + \text{Energy} \quad \text{(Eq.6)}$$

Estimates for the fractionation of NH_4^+ to NO_2^- range from -18 to -29‰ [1].

F. Denitrification

The denitrification is an effective method of removing NO_3^-, is part of the N-cycle transforms NO_3^- into N_2 gas. This is a reductive process and thus is a form of respiration, it occurs in four stages, NO_3^- to NO_2^-, NO_2^- to nitric oxide (NO), NO to N_2O and N_2O to N_2 [15].

Denitrifiers are commonly found in many natural environments such as soil, marine and freshwater sediment, as well in wastewater treatment systems. Occurs with a participation of heterotrophic and autotrophic bacteria. The genera *Pseudomonas, Ralstonia, Alcaligenes, Paracoccus, Rhodibacter, Rubrivivax, Thauera, Burkholdeira, Bacillus* and *Streptomyces* are the dominant denitrifiers in various environments [17].

Denitrification has large isotope fractionation effects due to the 'distillation' of N_2 gas. In shallow aquifers, N_2 gas produced by denitrification can be lost by diffusion to the atmosphere. This is a Rayleigh fractionation process with a large coefficient of fractionation. Measured fractionations for soil samples are often smaller -12 to -14‰ [1].

Denitrification is a process, in which we can see a large isotopic fractionation of N and O. It has a distinctive influence on the $\delta^{15}N$ values in nitrates: with decreasing NO_3^- concentrations, the $\delta^{15}N$ value grows exponentially[11][15].

G. Anaerobic ammonium-oxidizing (anammox)

Is an autotrophic biological process running under anaerobic conditions, in which a complete conversion of NH_4^+ to N_2 (without supplying an external organic C source). Microorganisms responsible for an Anammox process belong to three groups of bacteria: ***Brocadia*** (*B. anammoxidans and B. fulgida*), ***Kuenenia*** (*K.Stuttgartiensis*) and ***Scalindua*** (*S. wagneri, S. brodae, S. sorokinii*) [15].

We can observe the values of N Isotopic fractionation for the different stages of the N-cycle in the table 2.

Table 2. The values of Nitrogen isotopic fractionation $\varepsilon_{s/p,}$ for microbial cultures [11].

Process	**Reaction**	**Ɛs/p [‰]**
N2 fixation	$N_2 \rightarrow$Norg	-2 to +2 [‰]
NH_4^+assimilation	$NH_4^+ \rightarrow$ Norg	+14 to 27‰
NH_4^+oxidation (nitrification) Nitrite oxidation (nitrification)	$NH_4^+ \rightarrow NO_2^-$ $NO_2^- \rightarrow NO_3^-$	+14 to +38‰ -12.8‰
Nitrate reduction (denitrification) Nitrite reduction (denitrification) Nitrous oxide reduction (denitrification)	$NO_3^- \rightarrow NO_2^-$ $NO_2^- \rightarrow NO$ $N_2O \rightarrow N_2$	+13 to 30‰ +5 to +25‰ +4 to +13‰
Nitrate reduction (nitrate assimilation)	$NO_3^- \rightarrow NO_2^-$	+5 to +10‰

2.2.1.3. ANALYTICAL METHODS

N_2 is used for $^{15}N/^{14}N$ isotope ratio measurements, the standard is atmospheric N_2. Various preparation procedures have been described for the different nitrogen compounds. In the early days of N isotope investigations, the extraction and combustion techniques potentially involved chemical treatments that could have introduced isotopic fractionations. More recently, simplified techniques for combustion have come into routine use, so that a precision of 0.1-0.2‰ for $\delta^{15}N$ determinations can be achieved. Organic N-compounds are combusted to CO_2, H_2O and N_2 in an elemental analyzer. The cryogenically purified N_2 is trapped for analysis. More recently methods have been described that are based on the isotope analysis of N_2O. Measurements of bulk $\delta^{15}N$ values yield qualitative rather quantitative information on the N-cycle, special techniques are necessary for a separate analysis of nitrate and nitrite in samples containing both species [11]. Coplen et. al. [26] developed a method to measure N_2O generated by denitrifying bacteria lacking N_2O reductase.

2.2.2. ISOTOPIC FRACTIONATION PROCESSES OF CARBON

2.2.2.1. CARBON

The most important C forms in the biosphere are gaseous CO_2 and CH_4, dissolved CO_2 (carbonate species), solid carbonate minerals, and organic compounds [1]. The broad spectrum of C-bearing compounds involved in low and high temperature geological settings can be assessed based on carbon isotope fractionations [11].

The three major reservoirs for C on the Earth are sedimentary organic matter, the biosphere and sedimentary carbonates[4]. However, the abundance of CO_2 in the atmosphere is minuscule compared to the major reservoirs. Reservoirs, their abundance, fluxes, and their $\delta^{13}C$ values are given in Table 3 [1].

Table 3. Mass and Carbon isotope composition of major carbon reservoirs [1]

Reservoir	Mass/10^{15}g C	$\delta^{13}C$ ‰ (PDB) average
Atmosphere (290 PPM)	775	-6 TO -7
Ocean (TDC)	35 000	0
(DOC)	1 000	-20
(POC)	3	-22
Land plants	1600	-25 (-12 for C_4 plants)
Sedimentary inorganic C (carbonates)	**60 000 000**	0 to 1
Organic carbon	**15 000 000**	-23
Continental silicic crust	**7 000 000**	-6
Mantle	**324 000 000**	-5 to -6

2.2.2.2. CARBON CYCLE

The global atmospheric $\delta^{13}C$ value is related to the overall global C-cycle [1]. The C-cycle is the biogeochemical cycle by which C is exchange among the biosphere, pedosphere, geosphere, hydrosphere and atmosphere of the Earth. The C-cycle comprises a sequence of events that are key to make Earth capable of sustaining life. It describes the movement of C as it is recycled and reused throughout the biosphere, as well as long-term processes of C sequestration (Figure 3). Mayor biochemical C-cycle processes include photosynthesis or chemosynthesis, whereby CO_2 is converted into organic matter; respiration, whereby organic compounds are oxidized to CO_2; and methanogenesis and fermentation, which may be considered reduction of CO_2 to CH_4. The most important factor affecting C-isotopic compositions of natural compounds in the biosphere is the effect of absorption and photosynthetic fixation of CO_2 by plants [5].

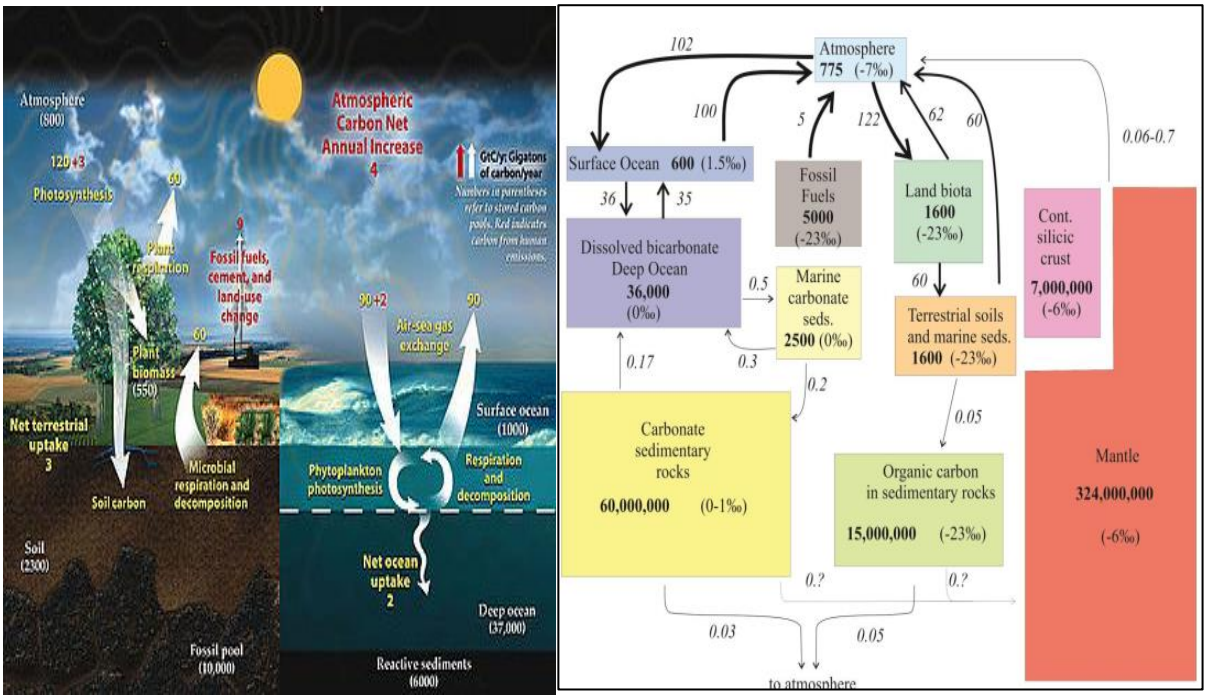

a) b)

Figure 3. a) Movement of carbon between land, atmosphre, and ocean in billions of tons per year. Yelow numbers are natural fluxes, red are human contributions, white are stored carbon. b) Carbon cycle showing fluxes and $\delta^{13}C$ values of different reservoirs. Abundance shown in bold in 10^{15}g. Flux shown in italics in 10^{15}g/yrs. $\delta^{13}C$ values are in parentheses [1][27].

Important biochemical transformations of C include:

- Respiration: C-org→CO_2
- Oxidation: CH_4→ CO_2
- Fermentation: C-org→CH_4
- Methanogenesis: CO_2→CH_4
- Fixation:CO_2→C-org
- Photosynthesis or Chemosynthesis [5].

2.2.2.3. ORGANIC CARBON SYSTEM (PHOTOSYNTHETIC PAHWAYS)

The different photosynthetic pathways were recognized by stable isotope geochemists based on distinct $\delta^{13}C$ values in plants [1]:

A. Photosynthesis: converts CO_2 to carbohydrates via metabolic pathways that provide energy to an organism. The formation of reduced organic carbon occurs by reduction of CO_2 during photosynthesis. Terrestrial plants derive their carbon from photosynthetic fixation of atmospheric CO_2, as does marine plankton. Other aquatic plants fix carbon from dissolved bicarbonate (HCO_3) [1]. The selective enrichment of one stable isotope over another creates distinct isotopic fractionations that can be measured and correlated with among oxygenic

phototrophs. The degree of carbon isotope fractionation is influenced by several factors, including the metabolism, anatomy, growth rate, and environmental conditions of the organism. Understanding these variations in C fractionation across species is useful for biogeochemical studies, including the reconstruction of paleoecology, plant evolution, and the characterization of food chains [28]. Photosynthesis by upland trees and northern grasses involves a net fractionation of about 19‰, whereas that by tropical grasses including maize involves a small fractionation of about 6‰. Additional biological mechanism for fractionation of C isotopes include microbial decay processes, such as the formation of CH_4 during anaerobic decomposition and of CO_2 during aerobic respiration [5].

B. Rubisco: The large fractionation of ^{13}C in photosynthesis is due to the carboxylation reaction, which is carried out by the enzyme ribulose-1,5-bisphosphate carboxylase oxygenase($C_5H_{12}O_{11}P_2$), or Rubisco process. Rubisco catalyzes the reaction between a five-C molecule, ribulose1,5-bisphosphate (RuBP) and CO_2 to form two molecules of 3-Phosphoglyceric acid (PGA). PGA reacts with NADPH (Nicotinamide adenine dinucleotide phosphate) to produce 3 phosphoglyceraldehide [1][29]. Isotope fractionation due to Rubisco carboxylation is predicted to be a 28‰ depletion, on average. However, fractionation values vary between organisms, ranging from an 11‰ depletion observed in cocolithophoric algae to a 29‰ depletion observed in spinach. Rubisco causes a kinetic isotope effect because $^{12}CO_2$ and $^{13}CO_2$ compete for the same active site and ^{13}C has an intrinsically lower reaction rate [30].

C. C_3 pathway : C_3 plants include rice, barley, wheat, cotton, spinach, potatoes. C_3 plants do not grow well in very hot or arid regions, uses carbon fixation (one of one of the three metabolic photosynthesis pathways which also include C_4 and CAM). These plants are called "C_3" due to the three-carbon compound (3-PGA) produced by the CO_2 fixation mechanism in these plants. This C_3 mechanism is the first step of the Calvin-Benson cycle, which converts CO_2 and Ribulose 1,5 bisphospate(RuB) into 3 PGA [1].

The isotope fractionations in C_3 carbon fixation arise from the combined effects of CO_2 gas diffusion through the stomata of the plant, and the carboxylation via Rubisco. Stomatal conductance discriminates against the heavier ^{13}C by 4.4‰. Rubisco carboxylation contributes a larger discrimination of 27‰ .The wide range of variation in delta values expressed in C_3 plants is modulated by the stomatal conductance or the rate of CO_2 entering, or water vapor exiting, the small pores in the epidermis of a leaf [31].

Rubisco enzyme catalyzes the carboxylation of CO_2 and the 5-carbon sugar, RuBP, into 3 phosphoglycerate, a 3-carbon compound through the following reaction (Eq.11):

$$CO_2 + H_2O + RuBP \rightarrow_{Rubisco} 2(3\text{-phosphoglycerate}) \quad (\text{Eq.11})$$

The product 3 phosphoglycerate is depleted in ^{13}C due to the kinetic isotopic effect of the above reaction. The typical range of C_3 plants is -33 to -23‰, with an overall ^{13}C fractionation for C_3 photosynthesis ranges between of –27 to –26‰ [1].

D. C_4 (dicarboxilic acid pathway): C_4 plants which use C_4 photosynthesis include grass, maize, sugar cane, millet and sorghum. C_4 plants have developed the C_4 carbon fixation pathway. C4 plants have high water efficiency, and so are tolerant to high temperatures and aridity conserve water loss, thus are more prevalent in hot, sunny, and dry climate [32].

Isotopic fractionation differs between C_4 carbon fixation and C_3, due to the spatial separation in C_4 plants of CO_2 capture (in the mesophyll cells) and the Calvin cycle (in the bundle sheath cells). In C_4 plants, carbon is converted to bicabonate fixed into oxaloacetate via the enzyme phosphoenolpyruvate (PEP) carboxilase and is then converted to malate. The malate is transported from the mesophyll to bundle sheat cells, which are impermeable to CO_2 [29]. The $\delta^{13}C$ values of C4 plants are about 13‰ higher than those of C_3 plants, ranging from -16 to -9‰, averaging -13 to -12‰ [1].

E. CAM (Crassulacean Acid Metabolism): Plants that use Crassulacean acid metabolism also known as CAM photosynthesis, are included in this group epiphytes (orchids, bromeliads) and xerophytes (succulents, cacti). Separate their chemical reactions between day and night. This strategy modulates stomatal conductance to increase water-use efficiency, so are well adapted for arid climates. In Crassulacean acid metabolism, isotopic fractionation combines the effects of the C_3 pathway in the daytime and the C_4 pathway in the night. This process alone is similar to that of C_4 plants and yields characteristic C_4 fractionation values of approximately -11‰.. During the day, CAM plants have approximately -28‰ fractionation, characteristic of C_3 plants These combined effects provide $\delta^{13}C$ values for CAM plants in the range of -10 to -20‰ [33].

F. Aquatic photosynthesis: aquatic organisms derive their carbon from dissolved carbon in water. Plankton get a significant portion of their carbon from dissolved CO_2. The $\delta^{13}C$ values of algae range from -22 to -10‰, plankton from -31 to -18‰, kelp from <-20 to -10‰. Most warm-water plankton have a $\delta^{13}C$ value of -22 to -17‰. It has been proposed that there is a temperature-dependent fractionation of the $\delta^{13}C$ value of plankton. When

molecular CO_2 is sufficiently abundant, there is constant fractionation of about 19‰ between CO_2 and cells over all reasonable temperatures. The average δ^{13}Cvalue of marine plants is ~ -20‰ [1].

2.2.2.4. CARBONATE SYSTEM

The fractionation during carbonate precipitation is small and relatively insensitive to temperature (unlike the oxygen isotope fractionation), so that δ^{13}C values of ancient marine carbonates (Fig 4) reflect the δ^{13}C value of dissolved inorganic carbon from which they formed Locally, and on relatively short timescales, the δ^{13}C value of dissolved inorganic carbon is related to productivity, ocean circulation, weathering, and input of carbon sources. Over the 10-100 million years scale, the global δ^{13}C value of dissolved inorganic carbon varies in relation to the relative proportions of the two major carbon reservoirs, organic carbon and carbonate in the crust [1].

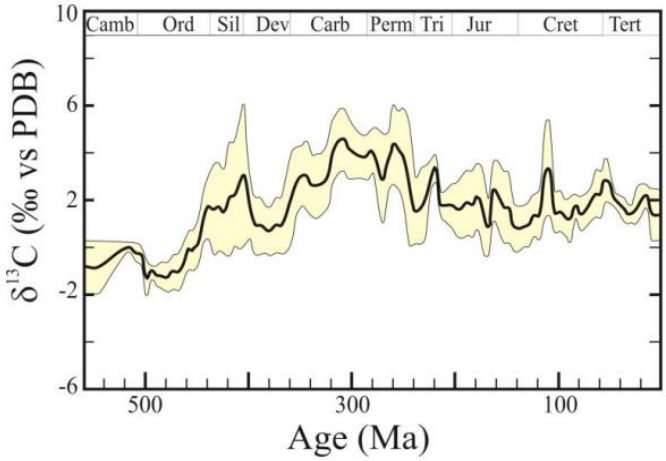

Figure 4. Secular variations of δ^{13}C variations in marine carbonates Data from low magnesium carbonate shells. The shaded area is 1σ uncertainty for a Gaussian Distribution [1].

The inorganic carbonate system is comprised of multiple chemical species linked by a series of equilibria (Eq.7, 8, 9):

$$CO_2\ (aq) + H_2O \leftrightarrow H_2CO_3 \quad \text{(Eq.7)}$$

$$H_2CO_3 \leftrightarrow H^+ \leftrightarrow HCO_3^- \quad \text{(Eq.8)}$$

$$HCO_3^- \leftrightarrow H^+ + CO_3^{2-} \quad \text{(Eq.9)}$$

The carbonate (CO_3^{2-}) ion can combine with divalent cations to form solid minerals, like calcite and aragonite (Eq. 10).

$$Ca^{2+} + CO_3^{2-} = CaCO_3 \quad \text{(Eq.10)}$$

An isotopic fractionation is associated with each of these equilibria, the ^{13}C differences between the species depend only on temperature, although the relative abundances of the species are strongly dependent on pH. The major problem in the experimental determination of the fractionation factor is the separation of the dissolved carbon phases (CO_2aq, HCO_3^- , CO_3^{2-}) because isotope equilibrium among these phases is reached within seconds. Another complicate factor is the shell carbonate precipitated by marine organisms which is frecuently not in equilibrium with the ambient dissolved bicarbonate [11].

2.2.2.5. ATMOSPHERIC CO_2

The average global $\delta^{13}C$ value of CO_2 in the atmosphere has changed from -6.7‰ in 1956 to –7.9‰, to less than -8.3‰ today as a result of fossil fuel burning. (The change is commonly referred to as the Suess Effect, although this term originally was used in the context of changing $\Delta^{14}C$ values due to the burning of 'dead' ^{14}C fossil fuels). Variations in the $\delta^{13}C$ values, of the atmospheric CO_2 before Keeling's work, at the Mauna Loa observatory have been measured using C_4 plants and particularly ice cores (Fig. 5). Ancient variations in atmospheric $\delta^{13}C$ are more difficult to determine but can be estimated from marine carbonates. The global atmospheric $\delta^{13}C$ value is related to the overall global carbon cycle [1].

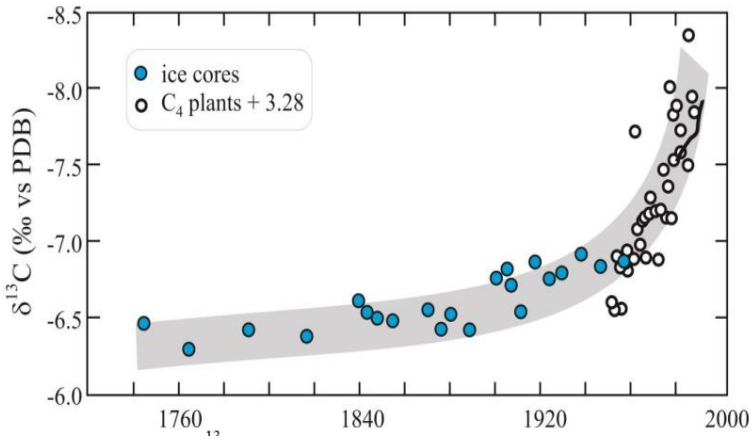

Figure 5. Variations in $\delta^{13}C$ value of atmospheric CO_2 as a function of age, data from direct measurements of atmospheric CO_2, measured $\delta^{13}C$ values of maize (C_4 plant) and ice core air inclusions [1].

2.2.2.6. ANALYTICAL METHODS

The gases used in $^{13}C/^{12}C$ measurements are CO_2 or CO obtained during pyrolysis. For CO_2 the following preparation methods exist:

- Carbonates are reacted with 100 % phosphoric acid (H_3PO_4) at temperatures between 20 and 90 °C (depending on the type of carbonate) to liberate CO_2.
- Organic compounds are generally oxidized at high temperatures (850–1000 °C) in a stream of oxygen or by an oxidizing agent like CuO. For the analysis of individual compounds in complex organic mixtures, a gas chromatography-combustion-isotope ratio mass-spectrometry (GC-C-IRMS) system is used. This device can measure individual carbon compounds in mixtures of sub-nanogram samples with a precision of better than ±0.5 ‰ [11].

2.3. PRINCIPLE OF ISOTOPE RATIO MASS SPECTROMETRY

Mass spectrometry methods are the most effective way of measuring isotope abundances. A mass spectrometer separates charged atoms and molecules based on their mases [11].

An Isotope ratio mass spectrometer consist of an inlet system, an ion source, an analyzer for ion separation, a detector for ion registration. The inlet system is designed to handle pure gases like CO_2, N_2. Neutral molecules from the inlet system are introduced in the ion source where they are ionized trough interaction with the electron beam and accelerated to several Kilovolts and the ions pass though the magnetic field before reaching the Faraday cup detectors (Fig. 6 and 7) [4]. The strength of the magnetic field and the accelerating voltage determine the trajectory of the ions and which ions enter the Faraday cups. Multiple collectors allow simultaneous measurement of ion intensity [34].

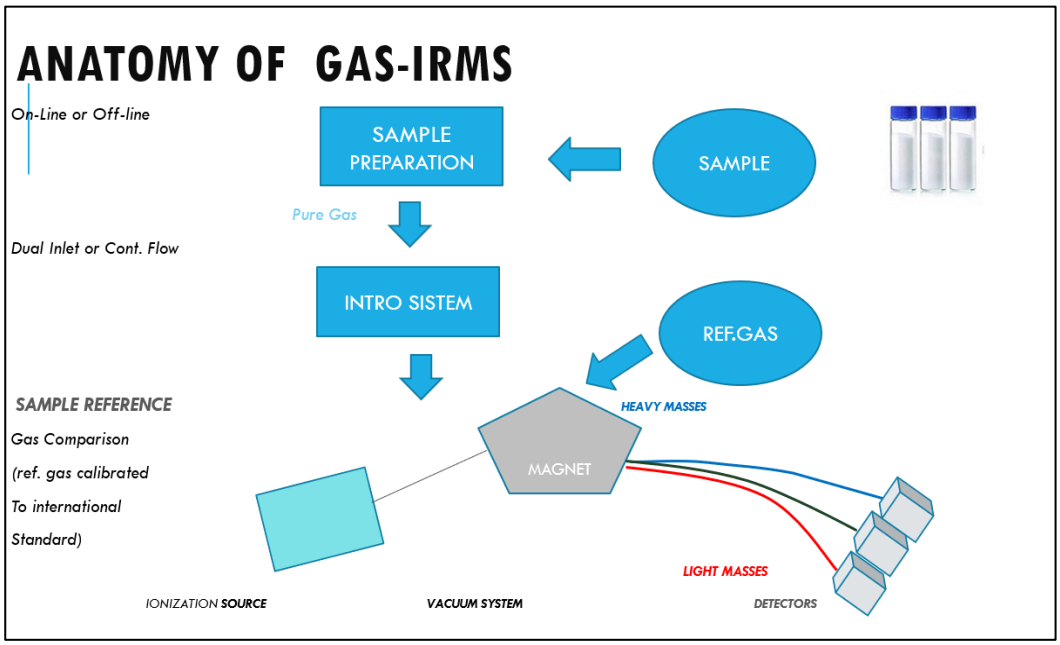

Figure 6. Anatomy of IRMS [35]

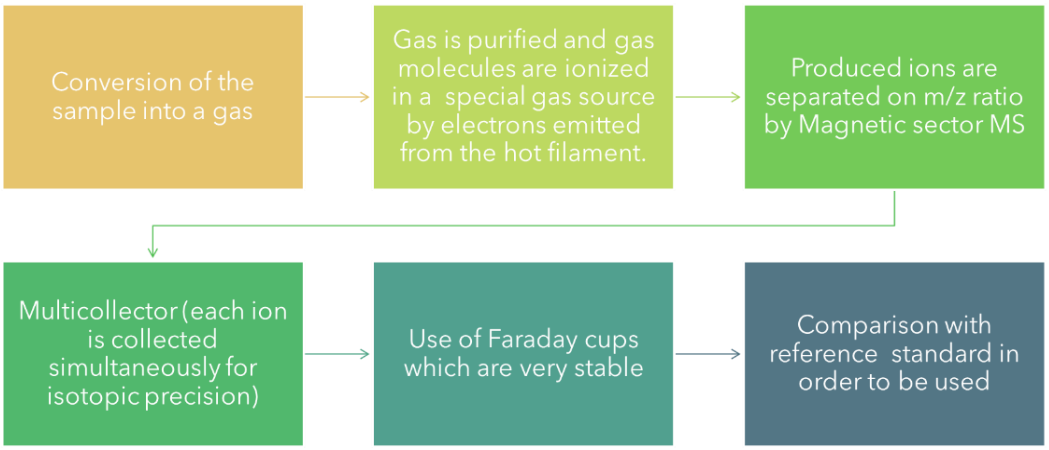

Figure 7. Principle of CF-IRMS [35]

2.4. CALIBRATION

The terminology calibration is more generally applied to calibration of the δ-scale rather than m/z scale. Calibration of the magnet is typically performed following software installation [34].

Reference materials for isotope ratio measurands are classified in:

- Primary (calibration materials)
- Secondary (reference materials)

2.4.1. Primary (calibration) materials

The primary materials currently kept and distributed by the International Atomic Energy Agency (IAEA) are listed in Table 4. At the present, a laboratory can receive a portion of each primary material will be available for several decades.

Table 4. The reference materials against which δ-scales are calibrated [34]

Primary reference material	**Nature**	**Isotopic ratio**	δ **‰**		**Scale**
VSMOW2	Water	$^{2}H/^{1}H$ $^{18}O/^{16}O$ $^{17}O/^{16}O$	0.00±0.3* 0.00±0.02 0.00±0.03		VSMOW VSMOW VSMOW
NBS-19	Calcium carbonate	$^{13}C/^{12}C$ $^{18}O/^{16}O$	+1.95* -2.20*		VPDB VPDB
	*There are no uncertainties associated with the δ-values of NBS-19.				

2.4.1.1. Atmospheric nitrogen δ -scale

The primary reference material for relative N isotope-ratio measurements ($\delta^{15}N$) is atmospheric N_2 which has $\delta^{15}N$ consensus value of 0 for all N isotope-ratio analysis as it does not vary

around the world or over time. The $\delta^{15}N$ scale is determined by analysing reference materials IAEA-N-1 and IAEA-N-2, which have been assigned values of +0.43‰ and +20.3‰, respectively [26].

2.4.1.2. The Vienna Peedee Belemnite (VPDB) δ-scale

All carbonate δ-values must be referenced to the international standard VDPB, the successor of PDB as PDB is exhausted. However, VDPB with $\delta\,^{13}C = 0$ and $\delta\,^{18}O = 0$ as one expected, does not exist. Instead standards exist that are related to this virtual. PDB and VPDB are virtually identical, but the use of VPDB as a reference implies that the measurements haven been calibrated through NBS19. PDB consisted of calcium carbonate from a Cretaceous belemnite from the Peedee formation in South Carolina. Carbon isotope ratios are determined on gaseous CO_2 and commonly are measured with a standard deviation of ±0.1‰ [4].

VPDB has isotopic ratios characteristic of marine limestone and is considerably enriched in ^{13}C with respect to organic carbon compounds. It is now recommended that $\delta\,^{13}C$ values of inorganic and organic materials are expressed relative to VPDB on a scale normalised by assigning a value of -46.6±0‰ to LSVEC lithium carbonate. In order to maintain consistency with the historical data, the VPDB scale is still used for reporting $\delta^{18}O$ values of carbonates [34].

2.4.1.3. Secondary (reference) materials

These are natural or synthetic compounds which have been carefully calibrated versus the primary calibration materials. The δ-values of these materials are agreed internationally, but in contrast to the calibration materials have uncertainty associated with the δ-values. Tables 5 and 6 list some of the materials distributed by IAEA for $\delta^{15}N$ and $\delta^{13}C$ [34].

Table 5. Secondary reference materials for $\delta^{15}N$ measurements [34].

Description	NIST RM	Nature	$\delta^{15}N$‰	SD
USGS-32	8558	Potassium nitrate	+180	1
USGS-26	8551	Ammonium sulphate	+53.7	0.4
USGS-41	8574	L-glutamic acid	+47.6	0.2
IAEA-N-2	8548	Ammonium sulphate	+20.3	0.2
IAEA-NO-3	8549	Potassium nitrate	+4.7	0.2
USGS-35	8569	Sodium nitrate	+2.7	0.2
IAEA-600		Caffeine	+1.0	0.2

IAEA-N-1	8547	Ammonium sulphate	+0.4	0.2
USGS-34	8568	Potassium nitrate	-1.8	0.2
USGS-40	8573	L-glutamic acid	-4.5	0.1
USGS-25	8550	Ammonium sulphate	-30.4	0.4

Table 6. Secondary reference materials for $\delta^{13}C$ measurements [34].

Description	**NIST RM**	**Nature**	**$\delta^{18}C$‰**	**SD**
USGS-41	8574	L-glutamic acid	+37.626	0.049
IAEA-CH-6	8542	Sucrose	-10.449	0.033
USGS-24	8541	Graphite	-16.049	0.035
IAEA-CH-3		Cellulose	-24.724	0.041
USGS-40	8573	L-glutamic acid	-26.389	0.042
IAEA-600		Caffeine	-27.771	0.043
NBS-22	8539	Oil	-30.031	0.043
IAEA-CH-7	8540	Polyethylene	-32.151	0.050
LSVEC*	8545	Lithium carbonate	-46.6	0.2
* It is recommended that $\delta^{13}C$ values of both organic and inorganic materials are expressed relative to VPDB on a scale normalized assigning a value of -46.6‰ to LSV Lithium carbonate.				

2.4.2. Sample preparation

It is fundamentally important that samples and reference materials are prepared and analysed in an Identical Treatment (IT) Principle.To determine the isotope ratios of a single chemical species, a separation step is necessary before the combustion/conversion process, either by off-line purification processes, or by coupling techniques such as GC-IRMS [34].

2.4.3. Validation

The validity depends on both accuracy and precision of the values obtained for $\delta^{15}N$ and $\delta^{13}C$. First, the measurement of the samples with the mass spectrometer must be demonstrated to be correct; second, the techniques used for sample preparation must be both accurate and precise. Accuracy in stable isotope mass spectrometry is only relative because samples are compared to a standard [8].

To achieve accreditation to ISO/IEC 17025 or other internationally recognized quality standards, analytical techniques must be validated. The validation process will depend on the nature of the samples to be analysed, the equipment and the parameters to be measured, all must be defined in the validation plan.

Parameters which should be assessed include:

- **Linearity:** this should be determined using real samples in addition to the working gas. Refers to the ability of the measurement procedure to produce values δ-values that are independent of the material analysed.
- **Stability:** the standard deviation determined over 10 pulses of working gas should be determined over a significant period.
- **Repeatability:** one day, one system, one analyst, several measurements
- **Within-laboratory reproducibility**: (several days, different persons, one system, several measurements (Eq.11, Eq.12).

$$\mathrm{SPooled} = \sqrt{\frac{(n_1-1)s_1^2+(n_2-1)s_2^2 \ +\cdots+(n_k-1)s_k^2}{n_1+n_2+\cdots+n_k-k}} \qquad \text{(Eq.11)}$$

Where:

K: number of samples

s_1, s_2: within group standard deviation

n_1, n_2: numbers of measurements

$$\mathrm{RSDPooled} = \sqrt{\frac{(n_1-1)RSD_1^2+(n_2-1)RSD_2^2 \ +\cdots+(n_k-1)RSD_k^2}{n_1+n_2+\cdots+n_k-k}} \qquad \text{(Eq.12)}$$

- **Reproducibility**: (several days, different persons, several system/laboratories)-target values should be a standard deviation equal to or less than 3.0 ‰ for δ^2H, 0.5 ‰ for δ^{18}O, and equal to or less than 0.3‰ for δ^{13}C and δ^{15}N.
- **Selectivity**: The laboratory shall use test and for calibration methods, including methods for sampling, which meet the needs of the customer and which are appropriate for the tests and for calibrations. When the customer does not specify the method to be used, the laboratory shall select appropriate methods that have been published either in international, regional or national standards. or by reputable technical organizations. or in relevant scientific texts or journals, or as specified by the manufacturer of the equipment.
- **Robustness**: the effects of varying instrument parameters (temperatures, flow rates) [6].

2.4.4. Uncertainty

The IRMS can measure natural isotopic ratio variations with an uncertainty better than 0.02‰. Large errors are typically introduced by sample treatment prior to IRMS analysis. The basic

rule for combining uncertainties is the square root of the sum of the squares (Eq. 13). It is not possible to use simple rules for combining uncertainties, as this requires the uncertainty components to be expressed in the same units as the measurement result.

$$\mathrm{Uc(y)}\sqrt{\mathrm{u(x_1)^2 + u(x_2)^2 + \cdots u(x_n)^2}} \qquad \text{(Eq.13)}$$

For isotope δ-scales that are defined by two points or where it is recommended to use two or more reference materials RM1 and RM2, was used the (Eq.14).

The equation for calculating the $\delta_{\text{ true (sample)}}$ for two reference materials RM1 and RM2 can be written as in (Eq.14):

$$\delta_{\mathrm{true(sample)}} = \delta_{\mathrm{true(RM1)}} + \left[\delta_{\mathrm{raw(sample)}} - \delta_{\mathrm{raw(RM1)}} * \frac{(\delta_{\mathrm{true(RM1)}} - (\delta_{\mathrm{true(RM2)}}}{\delta_{\mathrm{raw(RM1)}} - \delta_{\mathrm{raw(RM2)}}} \right] \qquad \text{(Eq.14)}$$

Since the terms $\delta_{\text{true (RM1)}}$ and $\delta_{\text{raw (RM1)}}$ appear twice in (Eq.12) is not possible to use the simple rules for combining uncertainties. The straightforward approach is to use a spreadsheet-base calculation such as Kragten [34].

3. EXPERIMENTAL PROCEDURE

This section specifies samples and procedures thoroughly.

3.1. MATERIALS AND EQUIPMENT

3.1.1. Samples used

- Historical data (2014-2020) collected from the IRMS Laboratory from the Department of Geology of University of Tartu (ANEX 1).
- PN338 36700 Acetanilide STD Thermoscientific Thermofisher BN 200689
- PN338 40022 Aspartic Acid STD Thermoscientific Thermofisher BN200865
- PN338 40019 Nicotinamide STD Thermoscientific Thermofisher BN200844

The mass % of reference materials are specified in the table:

Table 7: Mass % Reference materials (samples)

STD	N%	C%	O%	H%
Acetanilide C_8H_9NO	10.36	71.09	11.84	6.71
Aspartic Acid $C_4H_7NO_4$	10.52	36.09	48.01	5.30
Nicotinamide $C_6H_6N_2O$	22.94	59.01	13.10	4.95

3.1.2. Equipment

The personal from the IRMS Lab used this equipment for measure $\delta^{13}C$ and $\delta^{15}N$ of the three standards mentioned in the table 7.

The analytical apparatus consists of four units:

- **An automated sample extraction:** constructed to hold 31 samples and is furnished with a CTC an analytical combiPAL, robotic sampling arm by which the sample is send to the IRMS through a volatile water removal unit and water removal unit.
- **Computer software:** Thermo Scientific ISODAT 3.0 Software, which controls the Delta V Plus IRMS with Flash HT Element analyser connected via CONFLO IV. Software acquires the data from the IRMS and calculates delta values.
- **IRMS:** Thermo Scientific Delta V Plus CF-IRMS. It has a universal triple collector, consisting of two wide cups with a narrow cup in the middle. It is capable of simultaneously measure mass charge (m/z) of the of CO_2 and N_2 molecule 44,45, 46 and 28,29, simultaneously. The ion beams for these m/z values are as follows m/z 28=N_2=$^{14}N^{14}N$; m/z 29=N_2=$^{14}N^{15}N$; m/z 44=CO_2=$^{12}C^{16}O^{16}O$; m/z=45= $CO_{2=}$ $^{13}C^{16}O^{16}O$ primarily, and m/z 46= $CO_{2=}$$^{12}C^{16}O^{18}O$ [36].
- **Elemental analyser Combustion (for C and N analysis):** Solid substances and non-volatile liquids can be introduced using tin (for C/N analysis. The analyser consists of two reactor systems, a **combustion** reactor followed by a **reduction** reactor. Combustion takes place in an O_2 atmosphere, in quartz reactor to produce CO_2, NOx and H_2O. The reactor contains (Chromium oxide) Cr_2O_3 and CO_3O_4+Ag and its temperature are around 900-1050^oC but at combustion of tin capsules raises to 1800^oC. It is recommended to use quartz inserts or ash crucibles to collect the ash from tin capsules [34].

3.2. METHODOLOGY

From the repeatability of the data obtained during the 2014-2020 (6 years) from the IRMS of the Department of Geology which provide measured values for $\delta^{13}C$ and $\delta^{15}N$ for the three samples used, are obtained the expanded uncertainties (U) which are calculated using Excel by means of the Kragten spreadsheet suggested by Carter et.al [34]. Uncertainties of the different measurements for $\delta^{13}C$ and $\delta^{15}N$ Aspartic acid, Nicotinamide and Acetanilide are quantified

by means of a Kragten spreadsheet approach, including the consideration of correlations between individual input parameters to the model equation (Eq.12).

The values of the parameters required to calculate the result and the associated standard uncertainties are entered into the spreadsheet in column B and C, respectively. The formula used to calculate the result is entered in cell B8. Column B is then copied into columns D to H (one column for each parameter used in the calculation of δtrue(sample). The uncertainty given in cell C3 is added to cell D3, the uncertainty in the cell C4 is added to cell E4, and so on (cells highlighted in turquoise color). Cells D8 to H8 show recalculated values for δtrue(sample), including the effect of the uncertainty in the individual parameters. Row 9 shows the differences between the recalculated values and the original calculation for δtrue(sample) in cell B8. The standard uncertainty in δtrue(sample) (cell C8) is obtained by squaring the differences in row 9, summing then and then taking the square root.

The analysis of stability was carried out using the program QI MACROS 2020 and Excel, using the Control charts Wizard. And for the analysis of reproducibility was used Pooled standard deviation (Eq.11) and Relative standard deviation (Eq.12).

The personal of the IRMS Lab of Geology follows the procedure of Révész et.al. [36] to obtain the readings of $\delta^{15}N$, and the $\delta^{13}C$, of total N and C of the three solid samples. A Flash HT combustion elemental analyser (EA) was used to convert total N and C in the solid samples into N_2 and CO_2 gas. The gas is then introduced into the IRMS through a Thermo scientific CONFLO IV interface. The CONFLO IV interface is used for introducing sample, N_2, and CO_2 reference gases and helium for sample dilution into the IRMS. The IRMS is a Thermo-Scientific Delta V Plus CF-IRMS. It has universal triple collector, two wide cups with a narrow cup in the middle, it is capable of measuring mass charge (m/z) 28,29 or with a magnet current change 44,45,46, simultaneously.

4. RESULTS

4.1. ANALYSIS OF UNCERTAINTY

ASPARTIC ACID $\delta^{15}N$.

Calculation of uncertainty in δtrue(sample) arising from two-point scale calibration using a Kragten spreadsheet. RMS used for scale calibration:IAEAN1 and IAEAN2.

Reference $\delta^{15}N$ values for RMs: IAEAN1=+0.4±0.2‰, IAEAN2=+20.3±0.2‰

Measured $\delta^{15}N$ values for RMs:IAEAN1=+0.378±0.299‰, IAEA2=+20.338±0.1853 ‰

Measured $\delta^{15}N$ values for sample: -7.068± 0.628‰

Table 8: Calculation of $\delta^{15}N$ true (Aspartic acid) using the Kragten spread sheet.

1	A	B	C	D	E	F	G	H
2	Parameter	$\delta^{15}N$(‰)	u(‰)					
3	δtrue (IAEAN1)	0.4	0.2	0.6	0.4	0.4	0.4	0.4
4	δtrue (IAEAN2)	20.3	0.2	20.3	20.5	20.3	20.3	20.3
5	δraw (IAEAN1)	0.378	0.299	0.378	0.378	0.677	0.378	0.378
6	δraw (IAEAN2)	20.341	0.1853	20.341	20.341	20.341	20.526	20.341
7	δraw (sample)	-7.068	0.628	-7.068	7.068	7.068	7.068	-6.440
8	δtrue (sample)	**-7.0**	**0.8**	-6.7	-7.1	-7.4	-7.0	-6.4
9			Diference	0.3	-0.1	-0.4	0.1	0.6
10			Squared Diferences	0.08	0.01	0.17	0.005	0.39
11			SumSQ	0.65				
12			Unc.contr.	0.001%	1%	27%	1%	60%

From the Table 8: Result = $\delta^{15}N$ = -7.0±1.6‰, K=2, norm.

Standard uncertainty:0.8‰ level of confidence 68%

Expanded uncertainty: U=u*k: 1.6‰

K=coverage factor k=2 level of confidence 95%

The measurement result means the following: The true value of $\delta^{15}N$ in Aspartic acid is in the range -8.6…-5.4 ‰, with the approximate probability 95%

ASPARTIC ACID $\delta^{13}C$.

Calculation of uncertainty in δtrue (sample) arising from two-point scale calibration using a Kragten spreadsheet. RMS used for scale calibration:IAEACH3 and IAEACH6.

Reference $\delta^{13}C$ values for RMs: IAEACH3=-24.724±0.041‰, IAEACH6=-10.449.3±0.033‰

Measured $\delta^{13}C$ values for RMs:IAEANCH3=-24.672±0.176‰, IAEACH6=-10.467±0.1735 ‰

Measured $\delta^{13}C$ values for sample: +1.962± 14.205‰

Table 9: Calculation of $\delta^{13}C$ true (Aspartic acid) using the Kragten spread sheet.

1	A	B	C	D	E	F	G	H
2	Parameter	$\delta^{13}C$(‰)	u(‰)					
3	δtrue (IAEACH3)	-24.724	0.041	-49	-24.724	-24.724	-24.724	-24.724
4	δtrue (IAEACH6)	-10.449	0.033	-10.449	-10.416	-10.449	-10.449	-10.449
5	δraw (IAEACH3)	-24.672	0.176	-24.672	-24.672	-24.496	-24.672	-24.672
6	δraw (IAEACH6)	-10.467	0.173516	-10.467	-10.467	-10.467	-10.2935	-10.467
7	δraw (sample)	1.962	14.205	1.962	1.962	1.962	1.962	16.167
8	δtrue (sample)	**2.0**	**14.3**	2.0	2.1	2.2	1.7	16.3
9			Diference	-0.04	0.1	0.2	-0.3	14.3
10			Squared Diferences	0.001	0.004	0.02	0.10	203.78
11			SumSQ	203.91				
12			Unc.contr.	0.001%	0.002%	0.01%	0.1%	99.9%

From the Table 9: Result = $\delta^{13}C$ = 2.0±28.6‰, k=2, norm.

Standard uncertainty:14.3‰ level of confidence 68%

Expanded uncertainty: U=u*k: 28.6‰

K=coverage factor k=2 level of confidence 95%

The measurement result means the following: The true value of $\delta^{13}C$ in Aspartic acid is in the range -26.5…30.6 ‰, with the approximate probability 95%

NICOTINAMIDE $\delta^{15}N$.

Calculation of uncertainty in δtrue (sample) arising from two-point scale calibration using a Kragten spreadsheet. RMS used for scale calibration:IAEAN1 and IAEAN2.

Reference $\delta^{15}N$ values for RMs: IAEAN1=+0.4±0.2‰, IAEAN2=+20.3±0.2‰

Measured $\delta^{15}N$ values for RMs:IAEAN1=+0.382±0.29‰, IAEA2=+20.34±0.18069 ‰

Measured $\delta^{15}N$ values for sample: -2.067± 0.320487‰

Table 10: Calculation of $\delta^{15}N$ true (Nicotinamide) using the Kragten spread sheet.

1	A	B	C	D	E	F	G	H
2	Parameter	$\delta^{15}N$(‰)	u(‰)					
3	δtrue (IAEAN1)	0.4	0.2	0.6	0.4	0.4	0.4	0.4
4	δtrue (IAEAN2)	20.3	0.2	20.3	20.5	20.3	20.3	20.3
5	δraw (IAEAN1)	0.383	0.29	0.382	0.382	0.672	0.382	0.382
6	δraw (IAEAN2)	20.34	0.18069	20.34	20.34	20.34	20.52069	20.34
7	δraw (sample)	-2.067	0.320487	-2.067	-2.067	-2.067	-2.067	-1.747
8	δtrue (sample)	**-2.0**	**0.5**	-1.8	-2.1	-2.4	-2.0	-1.7
9			Diference	0.2	-0.02	-0.3	0.02	0.3
10			Squared Diferences	0.05	0.001	0.11	0.0005	0.10
11			SumSQ	0.26				
12			Unc.contr.	19%	0.2%	41%	0.2%	39%

From the Table 10: Result = $\delta^{15}N$: -2.0±1.0‰, K=2, norm.

Standard uncertainty:0.5‰ level of confidence 68%

Expanded uncertainty: U=u*k: 1.0‰

K=coverage factor k=2 level of confidence 95%

The measurement result means the following: The true value of $\delta^{15}N$ in Nicotinamide is in the range -3…-1 ‰, with the approximate probability 95%

NICOTINAMIDE $\delta^{13}C$.

Calculation of uncertainty in δtrue (sample) arising from two-point scale calibration using a Kragten spreadsheet. RMS used for scale calibration:IAEACH3 and IAEACH6.

Reference $\delta^{13}C$ values for RMs: IAEACH3=-24.724±0.041‰, IAEACH6=-10.449.3±0.033‰

Measured $\delta^{13}C$ values for RMs:IAEANCH3=-24.666±0.169‰, IAEACH6=-10.474±0.1676 ‰

Measured $\delta^{13}C$ values for sample: -34.418± 0.193‰.

Table 11: Calculation of $\delta^{13}C$ true (Nicotinamide) using the Kragten spread sheet.

1	A	B	C	D	E	F	G	H
2	Parameter	$\delta^{13}C$(‰)	u(‰)					
3	δtrue (IAEACH3)	-24.724	0.041	-24.683	-24.724	-24.724	-24.724	-24.724
4	δtrue (IAEACH6)	-10.449	0.033	-10.449	-10.416	-10.449	-10.449	-10.449
5	δraw (IAEACH3)	-24.664	0.171	-24.664	-24.664	-24.835	-24.664	-24.664
6	δraw (IAEACH6)	-10.474	0.169259	-10.474	-10.467	-10.467	-10.2935	-10.467
7	δraw (sample)	-34.418	0.193	-34.418	-34.418	-34.418	-34.418	-34.225
8	δtrue (sample)	**-34.5**	**0.4**	-34.5	-34.6	-34.2	-34.4	-34.3
9			Diference	0.1	0.02	0.3	0.1	0.2
10			Squared Diferences	0.005	0.001	0.08	0.01	0.04
11			SumSQ	0.14				
12			Unc.contr.	3%	0.4%	59%	10%	27%

From the table 11: Result= $\delta^{13}C$=-34.5±0.7‰, K=2, norm

Standard uncertainty:0.4‰ level of confidence 68%

Expanded uncertainty: U=u*k: 0.7‰

K=coverage factor k=2 level of confidence 95%

The measurement result means the following: The true value of $\delta^{13}C$ in Nicotinamide is in the range -35.8…-35.3 ‰, with the approximate probability 95%

ACETANILIDE $\delta^{15}N$.

Calculation of uncertainty in δtrue (sample) arising from two-point scale calibration using a Kragten spreadsheet. RMS used for scale calibration:IAEAN1 and IAEAN2.

Reference $\delta^{15}N$ values for RMs: IAEAN1=+0.4±0.2‰, IAEAN2=+20.3±0.2‰

Measured $\delta^{15}N$ values for RMs:IAEAN1=+0.382±0.292‰, IAEA2=+20.34±0.147949 ‰

Measured $\delta^{15}N$ values for sample: +1.08413± 0.399387‰.

Table 12: Calculation of $\delta^{15}N$ true (Acetanilide) using the Kragten spread sheet.

1	A	B	C	D	E	F	G	H
2	Parameter	$\delta^{15}N$(‰)	u(‰)					
3	δtrue (IAEAN1)	0.4	0.2	0.6	0.4	0.4	0.4	0.4
4	δtrue (IAEAN2)	20.3	0.2	20.3	20.5	20.3	20.3	20.3
5	δraw (IAEAN1)	0.382	0.292	0.382	0.382	0.674	0.382	0.382
6	δraw (IAEAN2)	20.324	0.147949	20.324	20.324	20.324	20.324	20.324
7	δraw (sample)	1.08413	0.399387	1.084	1.084	1.084	1.084	1.484
8	δtrue (sample)	**1.1**	**0.5**	1.3	1.1	0.8	1.1	1.5
9			Diference	0.2	0.01	-0.3	-0.01	0.4
10			Squared Diferences	0.04	0.00005	0.08	0.00003	0.16
11			SumSQ	0.28				
12			Unc.contr.	13%	0.02%	29%	0.01%	57%

From the table 12: Result = $\delta^{15}N$= 1.1±1.1‰, K=2, norm.

Standard uncertainty:0.5‰ level of confidence 68%

Expanded uncertainty: U=u*k: 1.1‰

K=coverage factor k=2 level of confidence 95%

The measurement result means the following: The true value of $\delta^{15}N$ in Acetanilide is in the range 2.2…0.05 ‰, with the approximate probability 95%

ACETANILIDE $\delta^{13}C$.

Calculation of uncertainty in δtrue (sample) arising from two-point scale calibration using a Kragten spreadsheet: RMS used for scale calibration:IAEACH3 and IAEACH6.

Reference $\delta^{13}C$ values for RMs: IAEACH3= -24.724±0.041‰, IAEACH6=-10.449.3±0.033‰

Measured $\delta^{13}C$ values for RMs:IAEANCH3=-24.666±0.168‰,IAEACH6=-10.474±0.1728 ‰

Measured $\delta^{13}C$ values for sample: -26.888± 0.382168‰.

Table 13: Calculation of $\delta^{13}C$ true (Acetanilide) using the Kragten spread sheet.

1	A	B	C	D	E	F	G	H
2	Parameter	$\delta^{13}C$(‰)	u(‰)					
3	δtrue (IAEACH3)	-24.724	0.041	-24.683	-24.724	-24.724	-24.724	-24.724
4	δtrue (IAEACH6)	-10.449	0.033	-10.449	-10.416	-10.449	-10.449	-10.449
5	δraw (IAEACH3)	-24.664	0.168	-24.664	-24.664	-24.496	-24.664	-24.664
6	δraw (IAEACH6)	-10.477	0.17283	-10.477	-10.477	-10.477	-10.3042	-10.477
7	δraw (sample)	-26.888	0.382168	-26.888	-26.888	-26.888	-26.888	-26.506
8	δtrue (sample)	**-27.0**	**0.4**	-26.9	-27.0	-27.2	-26.9	-26.6
9			Diference	0.05	-0.01	-0.2	0.03	0.4
10			Squared Diferences	0.002	0.00003	0.04	0.001	0.15
11			SumSQ	0.19				
12			Unc.contr.	1%	0.01%	21%	0.4%	78%

From the table 13: Result= $\delta^{13}C$=-27.0±0.9‰, K=2, norm

Expanded Standard uncertainty:0.4‰ level of confidence 68%

uncertainty: U=u*k: 0.9‰

K=coverage factor k=2 level of confidence 95%

The measurement result means the following: The true value of $\delta^{13}C$ in Acetanilide is in the range -27.8…-26.1 ‰, with the approximate probability 95%.

4.2. ANALYSIS OF STABILITY

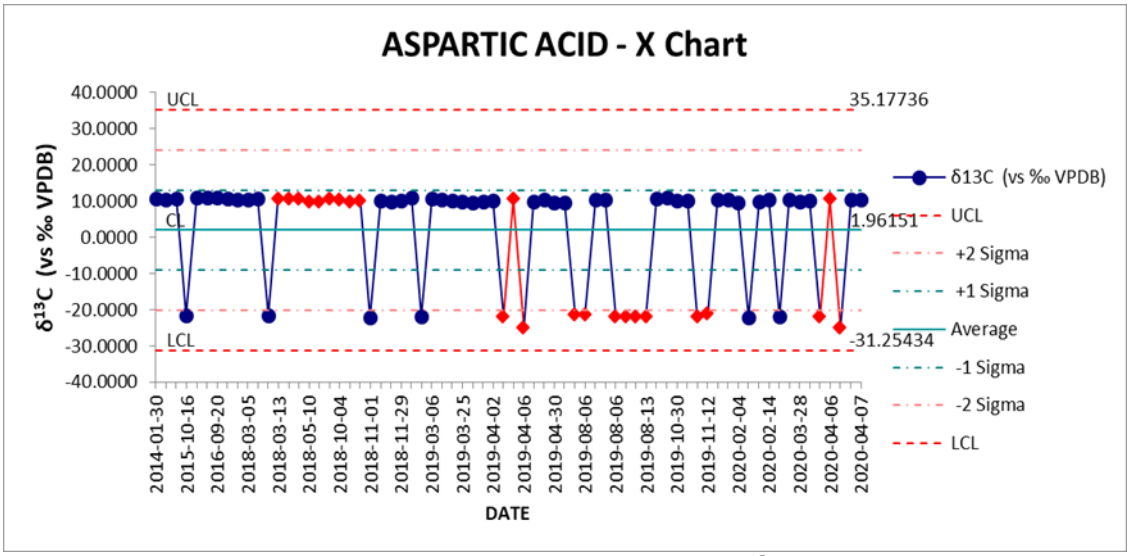

Figure 8. Stability Control chart -IRMS results $\delta^{13}C$ for Aspartic acid

The Figure 8 shows values for Nicotinamide $\delta^{13}C$ the UCL= 35.1774, +2σ= 24.1054, +1σ = 13.0335, average= 1.9615, -1σ= -9.1104, 2σ= -20.1824, LCL= -31.2543.

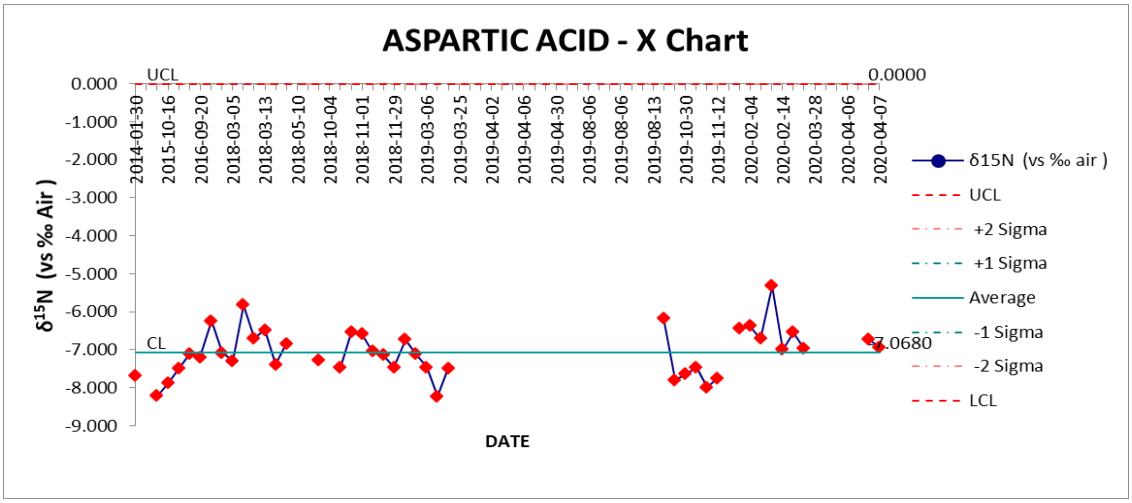

Figure 9. Stability Control chart -IRMS results $\delta^{15}N$ for Aspartic acid

The Figures 8 and 9 represent the analysis of stability for Aspartic acid, showing that for $\delta^{13}C$ have more stable measurements (blue points) with few unstable measurements (red points) between 2014- 2020. For $\delta^{15}N$ 99.7 % of the values are unstable between 2014 and 2020 all points are in red after stability analysis.

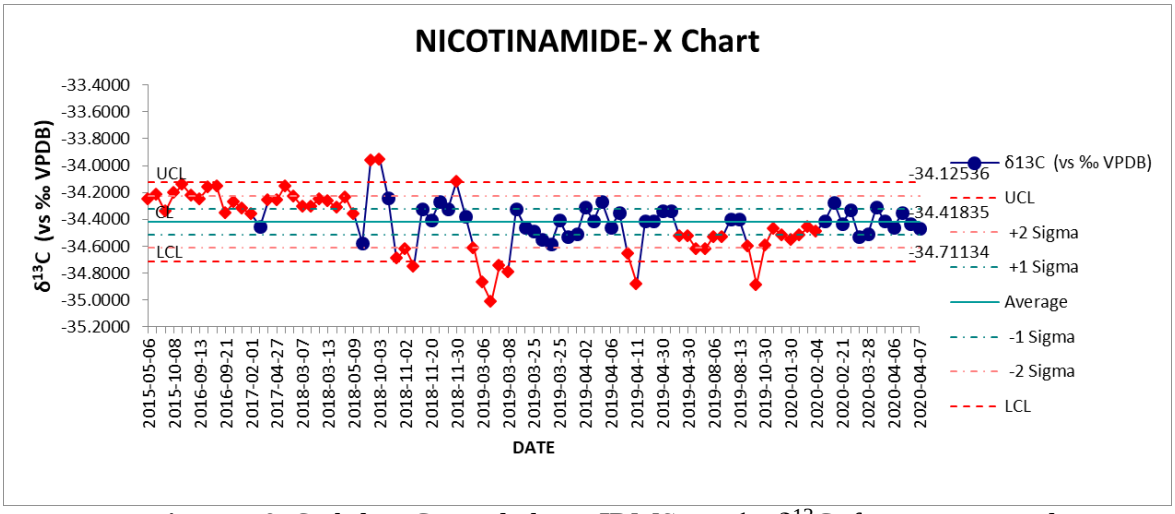

Figure 10. Stability Control chart -IRMS results $\delta^{13}C$ for Nicotinamide

The Figure 10 shows values for Nicotinamide $\delta^{13}C$ the UCL= -34.1254, +2σ= -34.2230, +1σ = -34.3207, average= -34.4184, -1σ= -34.5160, 2σ= -34.6137, LCL= -34.7113.

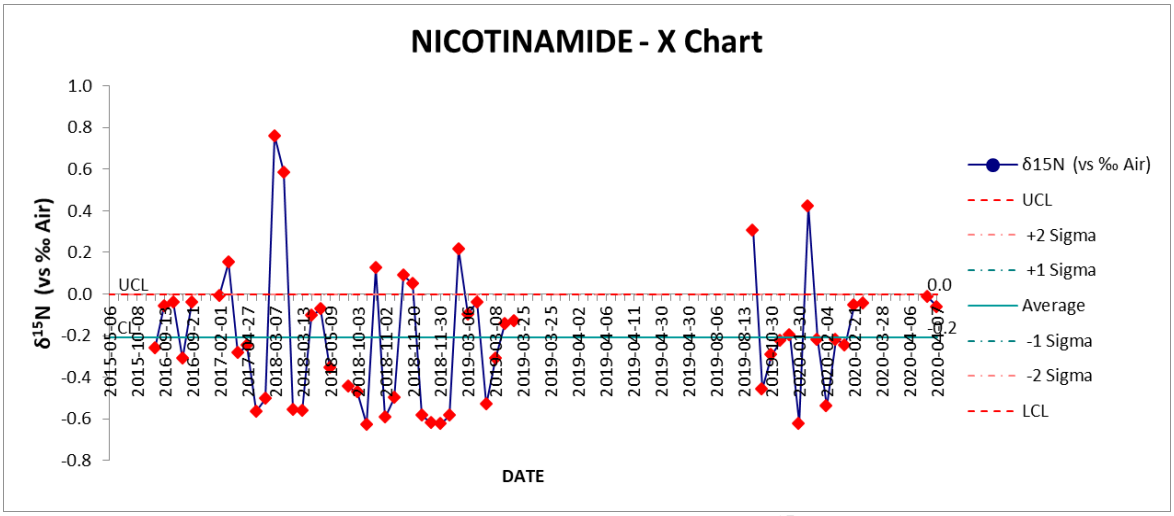

Figure 11. Stability Control chart -IRMS results $\delta^{15}N$ for Nicotinamide

The Figure 10 and 11 represent the analysis of stability for Nicotinamide, showing that for $\delta^{13}C$ values are more stable between the end of 2018, 2019 and 2020 (blue points) with several unstable points and outliners coming out from the upper and lower control limits, but it is more unstable at 2015 and at the beginning of 2018 with more outliners. For $\delta^{15}N$, 99.7 % of the values are unstable between 2015 and 2020 which are represented with red points in the Figure 11.

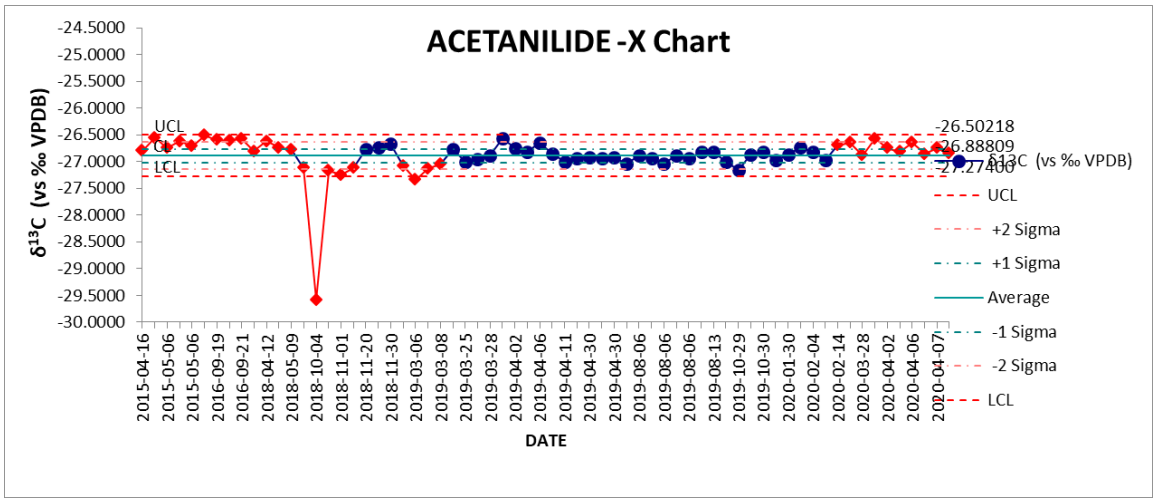

Figure 12. Stability Control chart -IRMS results $\delta^{13}C$ for Acetanilide

The Figure 12 shows values for $\delta^{13}C$ the UCL=-26.5022, $+2\sigma$= 2-26.6308, $+1\sigma$ =-26.7595, average= -26.8881, -1σ= -27.0167, 2σ= -27.1454, LCL=-27.2740.

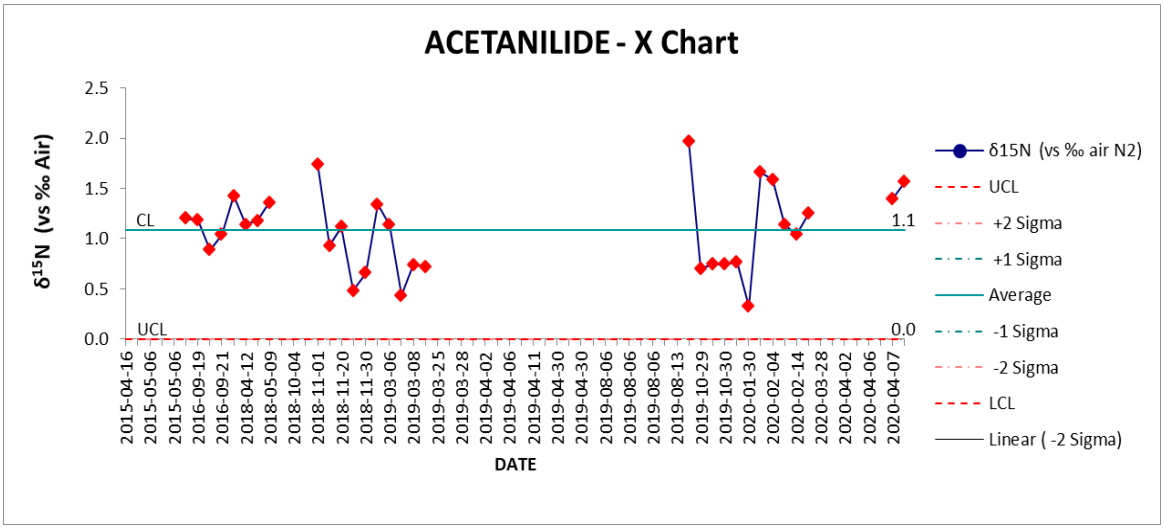

Figure 13. Stability Control chart - IRMS results $\delta^{15}N$ for Acetanilide

The Figure 12 and 13 represent the analysis of stability for Acetanilide, showing that for $\delta^{13}C$ values are more stable between the beginning of 2019 and the beginning of 2020 but several unstable points appearing in red during 2015, 2016, 2018 and 2020. For $\delta^{15}N$, 99.7% of values are unstable between 2015 and 2020 which is showed in the Figure 13 with the points in red.

4.3. ANALYSIS OF WITHIN LAB REPRODUCIBILITY(S_{RW})

For calculate within-laboratory long term reproducibility was used the Pooled Standard Deviation (Eq. 11) and Relative Pooled Relative Standard Deviation (Eq.12).

ASPARTIC ACID $\delta^{15}N$ (‰ vs Air)

Table 13: Pooled standard deviation for Aspartic acid $\delta^{15}N$ (‰ vs Air)

Date	2014	2015	2016	2017	2018	2019	2020
SD	0	0.23977	0.20336	0.59060	0.48667	0.58522	0.55227
DF (n.-1)	0	1	2	1	12	10	7
(n-1)*s^2	0	0.51906	0.05749	0.082711	2.842222	3.42485	2.135016
Rep.Pooled	0.52	‰					

Table 14: Relative pooled standard deviation for Aspartic acid $\delta^{15}N$ (‰ vs Air)

Date	2014	2015	2016	2017	2018	2019	2020
Mean	-7.681	-8.050	-7.271	-6.659	-6.926	-7.439	-6.57034
RSD	0	-0.02978	-0.02797	-0.08869	-0.07026	-0.07867	-0.08406
n-1* RSD^2	0	0.000887	0.001565	0.007866	0.059244	0.061894	0.049457
RSDPooled	0.07						
% RSD Pooled	7.00%						

ASPARTIC ACID $\delta^{13}C$ (‰ vs VPDB)

Table 15: Pooled standard deviation for Aspartic acid $\delta^{13}C$ (‰ vs VPDB)

Date	2014	2015	2016	2017	2018	2019	2020
SD	0	18.62056	0.125105	0.101973	10.97966	15.84421	15.05951
DF (n-1)	0	2	2	1	15	29	14
(n-1)*s^2	0	693.4502	0.031302	0.010399	1808.293	7280.126	3175.046
Rep.Pooled	14.34	‰					

Table 16: Relative pooled standard deviation for Aspartic acid $\delta^{13}C$ (‰ vs VPDB)

Date	2014	2015	2016	2017	2018	2019	2020
Mean	10.829	-0.141	10.999	10.561	6.246	-1.618	1.425
RSD	0	-132.008	0.011374	0.009656	1.757917	-9.7944	10.56655
n-1* RSD^2	0	34852.19	0.000259	9.32E-05	46.35409	2781.977	1563.129
RSDPooled	24.96						
% RSD Pooled	2496.00%						

ACETANILIDE $\delta^{15}N$ (‰ vs Air)

Table 17: Pooled standard deviation for Acetalinide $\delta^{15}N$ (‰ vs Air)

Date	2016	2017	2018	2019	2020
SD	0.145977	0	0.393737	0.442301	0.432684
DF (n-1)	3	0	7	9	7
(n-1)*s^2	0.063928	0	1.085202	1.760671	1.310509
Rep.Pooled	0.40	‰			

Table 18: Relative pooled standard deviation for Acetalinide $\delta^{15}N$ (‰ vs Air)

Date	2016	2017	2018	2019	2020
Mean	1.079	1.426	1.076	0.930	1.245
RSD	0.135281	0	0.366004	0.47582	0.347413
(n-1) * RSD^2	0.054903	0	0.937714	2.037644	0.844869
RSD Pooled	0.39				
% RSD Pooled	39.00%				

ACETANILIDE $\delta^{13}C$ (‰ vs VPDB)

Table 19: Pooled standard deviation for Acetanilide $\delta^{13}C$ (‰ vs VPDB)

Date	2015	2016	2017	2018	2019	2020
SD	0.100064	0.040804	0	0.840635	0.150244	0.111261
DF (n-1)	4	3	0	10	30	13
(n-1)*s^2	0.040051	0.004995	0	7.066669	0.677201	0.160928
Rep.Pooled	0.36	‰				

Table 20: Relative pooled standard deviation for Aspartic acid $\delta^{13}C$ (‰ vs VPDB)

Date	2015	2016	2017	2018	2019	2020
Mean	-26.686	-26.569	-26.802	-27.140	-26.927	-26.775
RSD	-0.00374974	-0.00154	0	-0.03097	-0.00558	-0.00416
(n-1) * RSD^2	5.62421E-05	7.08E-06	0	0.009594	0.000934	0.000224
RSD Pooled	0.013426					
% RSD Pooled	1.00%					

NICOTINAMIDE $\delta^{15}N$ (‰ vs Air)

Table 21: Pooled standard deviation for Nicotinamide $\delta^{15}N$ (‰ vs Air)

Date	2015	2016	2017	2018	2019	2020
SD	0	0.131844	0.20598	0.409438	0.242778	0.291379
DF (n-1)	0	3	3	20	11	9
(n-1)*s^2	0	0.052149	0.127284	3.352795	0.648354	0.764068
Rep.Pooled	0.33	‰				

Table 22: Relative pooled standard deviation for Nicotinamide $\delta^{15}N$ (‰ vs Air)

Date	2015	2016	2017	2018	2019	2020
Mean	-0.262	-0.112	-0.097	-0.293	-0.159	-0.160
RSD	0	-1.17244	-2.13325	-1.39727	-1.53164	-1.82536
(n-1) * RSD^2	0	4.123837	13.65228	39.04715	25.80497	29.9876
RSD Pooled	1.564663					
% RSD Pooled	156.00%					

NICOTINAMIDE $\delta^{13}C$ (‰ vs VPDB)

Table 23: Pooled standard deviation for Nicotinamide $\delta^{13}C$ (‰ vs VPDB)

Date	2015	2016	2017	2018	2019	2020
SD	0.064737993	0.093116631	0.091873978	0.205618	0.203853	0.090415
DF (n-1)	5	5	3	21	36	15
(n-1)*s^2	0.020955039	0.04340013	0.02532284	0.887858	1.496018	0.122624
Rep.Pooled	0.17	‰				

Table 24: Relative pooled standard deviation for Nicotinamide $\delta^{13}C$ (‰ vs VPDB)

Date	2015	2016	2017	2018	2019	2020
Mean	-34.229	-34.252	-34.332	-34.319	-34.538	-34.433
RSD	-0.00189132	-0.00272004	-0.00267604	-0.00599	-0.0059	-0.00263
(n-1) * RSD^2	1.78855E-05	3.69931E-05	2.14836E-05	0.000754	0.001254	0.000103
RSD Pooled	0.005073					
% RSD Pooled	1.00%					

5. DISCUSSION

- For the analysis of the uncertainty :

  Calculations of unceratinty are represented in tables 8 to 12, the Kragten spreadsheet was used to obtaing of the uncertainty of the Aspartic acid $\delta^{15}N$ is= -7.0±1.6 ‰ and for $\delta^{13}C$= is 2.0±28.6‰. For Nicotinamide the values are for $\delta^{15}N$= -2.0±1.0‰, and for $\delta^{13}C$= is -34.5±0.7‰. For Acetanilide the values for $\delta^{15}N$=1.1±1.1 ‰ and for $\delta^{13}C$ is -27.0±0.9‰. From these results we observe that the uncertainties of Nicotinamide and Acetanilide are ≤ ±1 ‰ for $\delta^{15}N$ and $\delta^{13}C$. This relatively low uncertainty is important for the precision of the $\delta^{15}N$ and $\delta^{13}C$ and it is a further demostration of the consistency of the fractionation.

- For the analysis of stability:

  Using wizard tool in QI Macros 2020, we could obtain the stability X-Charts that are represented in the Figures 8 to 13, we could observe very large stability for the measurements of $\delta^{13}C$ for Nicotinamide (-34.1254 to-34.7113) and Acetanilide (-26.5022 to -27.2740) but for Aspartic acid (+35.1774 to -31.2543) measurements are more unstable and outliners come out from the upper and control limits with means that some of these measurements were possibly manipulated or some other parameters are affecting these values ; for the values $\delta^{15}N$ in all three samples the values were unstable which are indicated with red points after using the analysis stability tool in QI Macros 2020.

- For precision (reproducibility) analysis:

  Within-laboratory long term reproducibility calculations are represented in the tables 13 to 24. For the Aspartic acid the %RSD pooled: $\delta^{15}N$= 7%, $\delta^{13}C$=2496%. For Acetalinide $\delta^{15}N$=39%, $\delta^{13}C$= 1%. For Nicotinamide $\delta^{15}N$=156% and $\delta^{13}C$= 1%. For these results we can observe that for Nicotinamide and Acetalinide the $\delta^{13}C$=1% which means that there is good precision in these measurements using the Delta V Plus CF-IRMS but for there is not precision for $\delta^{15}N$ in the three samples .

  The general pattern for $s_r < S_{RW} < u_c$

  Aspartic acid $\delta^{15}N$= 0.63 < 0.52< 0.8, $\delta^{13}C$=14.21 < 14.34 < 14.3
  Nicotinamide $\delta^{15}N$=0.32 < 0.33 < 0.5, $\delta^{13}C$=0.19 < 0.17 < 0.4
  Acetanilide $\delta^{15}N$=0.40 < 0.40 < 0.5, $\delta^{13}C$=0.38 < 0.36 < 0.4

  This patter shows good results for $\delta^{13}C$ Aspartic acid for Aspartic Acid, Nicotinamide and Acetanilide but not for $\delta^{15}N$ which confirms the stability of the three samples only for carbon.

6. CONCLUSIONS

- From the samples analysed using the combustion method the measurement uncertainty for Nicotinamide are for $\delta^{15}N$= -2.0±1.0‰, and for $\delta^{13}C$=-34.5±0.7‰, for Acetanilide the values for $\delta^{15}N$ are is 1.1±1.1 ‰ and for $\delta^{13}C$ is -27.0±0.9‰. These values shows that Nicotinamide and Acetalinide have significantly smaller uncertainties in comparison with Aspartic acid which values are for $\delta^{15}N$ = -7.0±1.6 ‰ and for $\delta^{13}C$ = 2.0±28.6‰.
- The analysis of stability of the Acetalinide (-26.5022 to -27.2740), Nicotinamide (-34.1254 to -34.7113), Aspartic acid (+35.1774 to -31.2543) shows more stability for the $\delta^{13}C$, but for $\delta^{15}N$ there is unstability during the years 2014-2020.
- For within lab reproducibility (S_{RW}) analysis for %RSD pooled for the Aspartic acid : $\delta^{15}N$= 7%, $\delta^{13}C$=2496%, for Acetalinide: $\delta^{15}N$=39%, $\delta^{13}C$= 1% and for Nicotinamide :$\delta^{15}N$=156% and $\delta^{13}C$= 1%. These results shows that for Nicotinamide and Acetalinide the $\delta^{13}C$=1% which means that there is good long term reproducibily in these measurements using the Delta V Plus CF-IRMS.
- It is possible that this large variability in Carbon and Nitrogen isotope values, results from fractionation that happened during sample preparation before the sample enter into the Delta V Plus CF-IRMS.

SUMMARY

ISOTOPIC STABILITY OF MASS REFERENCE MATERIALS AND POSSIBLE USE AS ISOTOPIC REFERENCE MATERIALS,

Margarita Esmeralda Gonzales Ferraz

Natural isotope variation or fractionation depends on equilibrium and kinetic processes affecting the individual isotope.

The purpose of the of this work is to determine the stability and reproducibility of historical data of $\delta(^{15}N/^{14}N)$ abbreviated as $\delta^{15}N$, and the $\delta(^{13}C/^{12}C)$, abbreviated as $\delta^{13}C$, of total N and C in three solid samples (Aspartic acid, Nicotinamide and Acetanilide). These three samples contain N and C. The primary reference material for relative N isotope-ratio measurements ($\delta^{15}N$) used were atmospheric nitrogen gas (N_2), which is widespread and homogeneous and by convention, has a $\delta^{15}N$ consensus value of 0‰. The primary reference material for relative C isotope-ratio measurements ($\delta^{13}C$) is the L-SVEC lithium carbonate which have consensus value of -46.6±0‰ on the Vienna Peedee Belemnite (VPDB scale. The secondary references used were IAEAN1 (+0.4±0.2‰), IAEAN2 (+20.3±0.2‰) for $\delta^{15}N$ and IAEACH3 (-24.724±0.041‰), IAEACH6 (-10.449±0.033‰) for $\delta^{13}C$.

The $\delta^{15}N$ and $\delta^{13}C$ data were provided for the Laboratory of Isotope Ration Mass Spectrometry (IRMS) of the Department of Geology University of Tartu. The $\delta^{15}N$ and $\delta^{13}C$ measurements were made with a Delta V Plus CF-IRMS, which alternately measures the isotope-amount ratios of the sample N_2 and CO_2 gases and one or more injections of the working reference N_2 and CO_2 gases.

From the data and results obtained for uncertainties for the data provided for the 2014-2020, we obtained the following results: for Aspartic acid $\delta^{15}N$ (-7.0±1.6 ‰), $\delta^{13}C$ (2.0±28.6‰), for Nicotinamide $\delta^{15}N$ (-2.0±1.0 ‰), $\delta^{13}C$ (-34.5±0.7‰) and for Acetanilide $\delta^{15}N$ (1.1±1.1 ‰), $\delta^{13}C$ (-27.0±0.9‰). These uncertainties probably could be due to fractionation process happening during sample preparation and transformation to gas before entering the IRMS.

From the analysis of the stability we can conclude that the Aspartic acid (+35.1774 to -31.2543), Nicotinamide (-34.1254 to-34.7113) and Acetanilide (-26.5022 to -27.2740) are more stable for $\delta^{13}C$, but unstable for $\delta^{15}N$ during, during 2014-2020. Lastly there is a good long-term reproducibility (S_{RW}) only for Acetanilide and Nicotinamide with % RSD pooled of 1% for $\delta^{13}C$.

Keywords: Nitrogen, Carbon, Fractionation, CF-IRMS.

CERCS code:

Kokkuvõte

MASSIETALONMATERJALIDE ISOTOOPSTABIILSUS JA ISOTOOPMATERJALIDENA KASUTAMISE VÕIMALUS,

Margarita Esmeralda Gonzales Ferraz

Isotoopide fraktsioneerumine looduslikes protsessides sõltub erinevates tasakaalu- ja kineetilisetest protsessidest.

Käesoleva töö eesmärgiks oli selgitada kolme Tartu Ülikooli geoloogi osakonna isotoopsuhte massispektroskoopia laboris elementanalüüsi C ja N referentsmaterjalide isotoopkoostise stabiilsus ja võimalik kasutatavus isotoopsuhte referentsmaterjalidena kasutades Kragteni tabelit. Kasutatud materjalid olid aspartaamhape, nikotiinamiid ja atsetaliniid. Lämmastiku isotoopkoostise ($\delta^{15}N$) peamine etalon onon homogeenne atmosfääri lämmastikugaas (N_2) mille puhul on kokkuleppe kohaselt $\delta^{15}N$ konsensusväärtus 0‰. Süsiniku isotoopide suhte mõõtmiste ($\delta^{13}C$) puhul on orgaanilise süsiniku materjalide puhul on L-SVEC liitiumkarbonaat, mille konsensus väärtus Viini Peedee Belemniidi skaalal on -46,6‰. Teisesed orgaaniliste ainete isotoopkoostise referentsmaterjalid on viited olid IAEAN1 (+0,4±0,2‰), IAEAN2 (+20,3±0,2‰) $\delta^{15}N$ ja IAEACH3 (-24,724 ± 0,041‰), IAEACH6 (-10,449±0,033‰) $\delta^{13}C$ puhul.

Kasutatud andmed saadi Tartu Ülikooli geoloogia osakonna isotoopide massispektromeetria laborist(IRMS) kus $\delta^{15}N$ ja δ13C mõõtmised tehti Delta V Plus CF-IRMS iga. Aastatel 2014–2020 saadud andmete analüüs näitab, et aspartaamhappe lämmastiku ja süsiniku stabiilsete isotoopide koostis on vastavalt $\delta^{15}N$ (-7,0±1,6 ‰) ja $\delta^{13}C$ (2,0±28,6‰). Nikotiinamiidi väärtused on $\delta^{15}N$ (-2,0±1,0 ‰) ja $\delta^{13}C$ (-34,5±0,7‰). Viimasega sarnaselt on atseetaaliniidi $\delta^{15}N$ väärtused 1,1±1,1 ‰ ja $\delta^{13}C$ väärtused -27,0±0,9‰. Aspartaamhappe suurtes piirides varieeruv isotoopkoostis võib olla tingitud fraktsioneerimisest proovide ettevalmistamise ja termilise lagundamise käigus

Stabiilsuse analüüsipõhjal võib järeldada, et asagiinhape (+35.1774 kuni -31.2543), nikotiinamiid (-34.1254 kuni-34.7113) ja atseetniiliid (-26.5022 kuni -27.2740) on δ13C puhul stabiilsemad, aastatel 2014–2020. Lõpuks on hea pikaajaline reprodutseeritavus (SRW) atseetniiliidi ja nikotiinamiidi puhul, kusjuures RSD % on 1% δ13C puhul.

Märksõnad: lämmastik, süsinik, fraktsioneerimine, CF-IRMS.

CERCS-kood:

REFERENCES

1. Sharp, Z., 2017. *Stable Isotopic Geochemistry*. Second Edition. Pearson, USA.
2. Rundel, P.W.,Enleringer.J.R., Nagy, K.A; 1989. *Stable Isotopes in Ecological Research*. Springer, New York.
3. Böhlke, J.K., Coplen, T. B., 1995. Interlaboratory Comparison of Reference Materials for Nitrogen-Isotope-Ratio Measurements.in Reference and intercomparison materials for stable isotopes of light elements. Vienna, *International Atomic Energy-IAEATECDOC*-825:51-66.
4. Martma, T., 2006. *Application of Carbon Isotopes to the study of the Ordovician and Silurian of the Baltic*. Press, Tallin.
5. Cravotta, Ch. A., 1997.*Use of Stable Isotopes of Carbon, Nitrogen and Sulfur to identify sources of Nitrogen in surface waters in the lower Susquehanna River Basin, Pennsylvania. U.S. Geological Survey*. Washington DC.
6. ISO/IEC 17025:2005. General Requirements for the competence of testing and calibration laboratories. *Bureau of Indian Standards*, New Delhi.
7. International Atomic Energy Agency 1998. *Stable Isotopes*, https://www.iaea.org/topics/nuclear-science/isotopes/stable-isotopes (last viewed 23.07.20)
8. Kreitler, Ch.W., 1975. Determining the Source of Nitrate in Ground Water by Nitrogen Isotopic studies. Report of Investigation No. 83:57. *Bureau of Economic Geology*. Austin, Texas.
9. Coplen, T.B., Herczeg, A.L., Barnes, C.J., 2000. Isotope Engineering-using Stable Isotopes of the Water Molecules to Solve Practical Problems. *Environmental Tracers in Subsurface Hydrology*., 79-110.
10. Clayton, R. N., Cole, D.R., Criss, R.E., Gregory, R.T., Kyser, T.K., Muehlenbanchs, K., Ohmoto, H., O'Neil,J., Sheppard, S.M., Taylor, B. E., Taylor, H.P., Walley, J.W., 1986. *Stable Isotopes in High Temperature*. Mineralogical Society of America, Virginia.
11. Hoefs, J., 2015. *Stable Isotope Chemistry.* Springer, Germany
12. Ryabenko, E., 2013.*Topics in Oceanography. Stable Isotope Methods for the Study of the Nitrogen Cycle*. Intech, Croatia.
13. Mariotti, A., Germon, J.C., Hubert, P., Kaiser, P., Letolle, R., Tardieux, A., Taridieux, P., 1981. Experimental determination of nitrogen kinetic isotope fractionation: Some principles; illustration for the denitrification and nitrification processes. *Plant and soil*., 62:413-430.
14. Roberston G & Groffman P 2015, *Nitrogen transformations*, Fourth Edition. Academic Press. USA.
15. Gebus, B., Halas, S., 2015. Isotopic Studies of Nitrates-A short review. Annales UMCS. *Physica*., 1:20-031.
16. Joo, Y.J., Li, D.D., Lerman, A., 2012. Global Nitrogen Cycle: Pre-Anthropocene Mass and Isotope Fluxes and the Effects of Human Perturbations. *Aquatic Geochemistry*., 19:477-500.
17. Bothe, H., Ferguson, S.J., Newton, W.E., 2007. *Biology of the Nitrogen Cycle*. Elsevier, UK.

18. Ottow, J.C., Benckiser, G., 1993. Effect of ecological conditions on total denitrification losses and N_2O release from soils, in The Terrestrial Nitrogen Cycle as Influenced by Man. *Nova Acta Leopoldina.*, 228:11-26.

19. Encyclopedia Britannica 2019. *Nitrogen Cycle*, https://www.britannica.com/science/nitrogen-cycle (last viewed 15.10.2019)

20. Sprent, J., 2005. *Nitrogen in soils.* ScienceDirect, https://www.sciencedirect.com/topics/agricultural-and-biological-sciences/nitrogen-fixing-bacteria (last viewed 30.10.2019)

21. Nieder, R., Benbi, D., 2008. *Carbon and Nitrogen in the terrestrial Environment*. Springer, Singapore.

22. Galloway, J.N., Dentener, F.J., Capone, D.G., Boyer, E.W., Howarth, R.W., Seitzinger, S.P., Asner, G.P., Cleveland, C.C., Green, P.A., Holland, E.A., Karl, D.M., Michaels, A.F., Porter, J.H., Townsend, A.R., Vöosmarty, C.J., 2004. Nitrogen Cycles: Past, Present and Future. *Biochemistry*., 70:153-226.

23. Andren, O., Lindberg, T., Paustian, K., Rosswall, T., 1990. *Ecology of Arable Land-Organisms Carbon and Nitrogen Cycling.* Ecological Bulletins 40, Sweden.

24. Troeh, F.R., Thompson, L.M., 2005. *Soils and Soil Fertility*. Sixth Edition. Blackwell Publishing, USA.

25. Park, S., Bae, W., Chung, J., Baek, S., 2007. Empirical model of the pH dependence of the maximum specific nitrification rate. *Process Biochemistry*., 42:1671-1676.

26. Coplen, T.B., Haiping, Q., Révész, K., Casciotti, K., Hannon, J.E., 2012. *Methods of the Reston Stable Isotope Laboratory. Determination of the $\delta^{15}N$ and $\delta^{18}O$ of Nitrate in Water. RSIL Lab Code 2900*. U.S. Geological Survey, Virginia.

27. Wikipedia 2020. *The Carbon Cycle*, https://en.wikipedia.org/wiki/Carbon_cycle (last viewed 25.07.20)

28. Fry, B., Sherr, E.B., 1989. $\delta^{13}C$ Measurements as Indicators of Carbon Flow in Marine and Freshwater Ecosystems. *Stable Isotopes in Ecological Research*., 68:196-229.

29. Hayes, J., 2001. Fractionation of Carbon and Hydrogen Isotopes in Biosynthetic Processes. *Reviews in Mineralogy and Geochemistry*.43(1):225-227.

30. McNevin, D.B., Badger, M. R., Whitney, S. M., Von Caemmerer, S., Tcherkez, G.B., Farquhar, G. D., 2007. .Differences in Carbon Isotope Discrimination of Three Variants of D-Ribulose-1,5-bisphosphate Carboxylase/Oxygenase Reflect Differences in Their Catalytic Mechanisms. *The Journal of Biology Chemistry*.282:36068-36076.

31. Whitehead, M.; 2017. *Environment and the state*. John Wiley & Sons, UK.

32. Kennedy, R. A., 1976. Photorespiration in C_3 and C_4 Plant Tissue Cultures. Significance of Kranz Anatomy to Low Photorespiration in C_4 Plants. *Plant Physiology* . 58(4):573-575

33. Wikipedia 2020. *Fractionation of carbon isotopes in oxygenic photosynthesis.* https://en.wikipedia.org/wiki/Fractionation_of_carbon_isotopes_in_oxygenic_photosynthesis (last viewed 23.07.20)

34. Carter, J.F., Barwick, V.J., 2011. Good Practice Guide for isotope Ratio Mass Spectrometry. *FIRMS*.ISBN 975-0-948926-31-0.UK

35. Univeristà del Salento 2020. *Fundamental of Stable Isotope Ratio Mass Spectrometry and Applications to measurements of water*. CEDAD, https://www.youtube.com/watch?v=afausciiKJM (last viewed 02.03.2020)

36. Révész, K., Haiping, Q., Coplen, T.B., 2012. *Determination of $\delta^{15}N$ and $\delta^{13}C$ of Total Nitrogen and carbon in solids. RSIL Lab Code 1832*. U.S. Geological Survey, Virginia.

ANNEX 1. EA-IRMS REFERENCE MATERIAL ISOTOPE DATA

date	Identifier 1	Row	Ampl. 29	d 15N/14N ref	calc N	Ampl. 44	d 13C/12C ref	calc C
4/24/2014	Acetanilide	2				8161	-26.724	-27.755
4/16/2015	Acetanilide	2	4769	1.843		8572	-26.914	-26.800
4/16/2015	Acetanilide	3	6066	2.041		10592	-26.667	-26.553
5/6/2015	Acetanilide	6				9603	-26.843	-26.748
5/6/2015	Acetanilide	7				12092	-26.710	-26.615
5/6/2015	Acetanilide	3				9848	-26.806	-26.711
9/13/2016	Acetanilide	6	8864	5.281	1.203		-27.005	-26.509
9/19/2016	Acetanilide	5	8008	4.323	1.183		-27.083	-26.589
9/20/2016	Acetanilide	5	8325	4.084	0.889		-27.119	-26.599
9/21/2016	Acetanilide	5	8607	4.443	1.041		-27.076	-26.578
2/1/2017	Acetanilide	6	6477	4.826	1.426	7482	-48.459	-26.802
4/12/2018	Acetanilide	6	5083	3.204	1.138	9449	-26.352	-26.622
5/9/2018	Acetanilide	7	5189	4.712	1.177	9805	-26.381	-26.734
5/9/2018	Acetanilide	8	4994	4.893	1.361	9507	-26.424	-26.777
5/10/2018	Acetanilide	5	4087	5.896		8449	-26.533	-27.122
10/4/2018	Acetanilide	6	12389	3.773		12957	-29.098	-29.581
10/4/2018	Acetanilide	7	3184	5.754		6164	-26.690	-27.169
11/1/2018	Acetanilide	6	3036	3.457	1.740	5608	-26.782	-27.247
11/2/2018	Acetanilide	6	3696	3.978	0.932	6812	-26.673	-27.122
11/20/2018	Acetanilide	6	6356	3.180	1.117	10974	-26.368	-26.766
11/29/2018	Acetanilide	6	5488	3.981	0.481	9598	-26.473	-26.727
11/30/2018	Acetanilide	6	5845	4.232	0.661	10176	-26.472	-26.671
3/6/2019	Acetanilide	6	5647	2.235	1.339	10198	-26.324	-27.075
3/6/2019	Acetanilide	34	4833	2.032	1.135	8945	-26.587	-27.342
3/8/2019	Acetanilide	6	4755	1.969	0.435	7961	-26.344	-27.124
3/8/2019	Acetanilide	31	5449	2.272	0.741	9085	-26.273	-27.053
3/22/2019	Acetanilide	6	5406	0.651	0.722	10417	-26.443	-26.771
3/25/2019	Acetanilide	6	5540	0.558		10770	-26.398	-26.998
3/25/2019	Acetanilide	30	5763	0.952		11123	-26.354	-26.954
3/28/2019	Acetanilide	6	6087	1.991		10947	-26.183	-26.885
3/28/2019	Acetanilide	52	7855	1.703		13820	-25.866	-26.569
4/2/2019	Acetanilide	6	5641	1.778		10401	-26.144	-26.742
4/2/2019	Acetanilide	81	5753	2.156		10810	-26.146	-26.811
4/6/2019	Acetanilide	6	5771	2.060		10698	-26.188	-26.648
4/6/2019	Acetanilide	70	6197	3.625		12024	-26.730	-26.857
4/11/2019	Acetanilide	5	4309	2.841		8387	-26.372	-27.013
4/30/2019	Acetanilide	6	4445	2.546		8641	-26.336	-26.944
4/30/2019	Acetanilide	47	4872	2.961		9380	-26.308	-26.916
4/30/2019	Acetanilide	6	4445	2.546		8641	-26.336	-26.944
4/30/2019	Acetanilide	47	4872	2.961		9380	-26.308	-26.916
8/6/2019	Acetanilide	6				7819	-26.524	-27.036
8/6/2019	Acetanilide	7				9520	-26.373	-26.884
8/6/2019	Acetanilide	47				9697	-26.426	-26.937
8/6/2019	Acetanilide	6				7819	-26.524	-27.036
8/6/2019	Acetanilide	7				9520	-26.373	-26.884
8/6/2019	Acetanilide	47				9697	-26.426	-26.937
8/13/2019	Acetanilide	6				8010	-26.345	-26.816
8/13/2019	Acetanilide	6				8010	-26.345	-26.816
10/29/2019	Acetanilide	6	5582	2.392	1.969	9210	-26.152	-27.001
10/29/2019	Acetanilide	49	5624	1.122	0.700	9472	-26.341	-27.161
10/30/2019	Acetanilide	5	5711	0.694	0.745	9713	-26.464	-26.877
10/30/2019	Acetanilide	48	6158	0.686	0.743	10389	-26.400	-26.813
11/12/2019	Acetanilide	6	5547	0.535	0.767	9632	-26.522	-26.969
1/30/2020	Acetanilide	7	5721	0.473	0.326	11872	-26.223	-26.868
1/30/2020	Acetanilide	49	6946	1.781	1.660	14301	-26.092	-26.737
2/4/2020	Acetanilide	5	5476	2.764	1.587	11895	-26.179	-26.825
2/4/2020	Acetanilide	39	4988	2.810	1.139	10800	-26.326	-26.970
2/14/2020	Acetanilide	7	6697	1.665	1.039	14355	-26.257	-26.694
2/21/2020	Acetanilide	7	6861	1.959	1.255	14767	-26.118	-26.641
3/28/2020	Acetanilide	6	6087	1.991		10947	-26.183	-26.885
3/28/2020	Acetanilide	52	7855	1.703		13820	-25.866	-26.569
4/2/2020	Acetanilide	6	5641	1.778		10401	-26.144	-26.742
4/2/2020	Acetanilide	81	5753	2.156		10810	-26.146	-26.811
4/6/2020	Acetanilide	6	5771	2.060		10698	-26.188	-26.648
4/6/2020	Acetanilide	70	6197	3.625		12024	-26.730	-26.857
4/7/2020	Acetanilide	7	5906	2.127	1.391	12902	-26.150	-26.747
4/7/2020	Acetanilide	41	5290	2.300	1.566	11763	-26.252	-26.849

1/30/2014	Aspartic Acid	4	4958	-6.175	-7.681	4648	10.049	10.829
10/8/2015	Aspartic Acid	5					10.627	10.443
10/16/2015	Aspartic Acid	2	5659	-6.737	-8.220		10.684	10.775
10/16/2015	Aspartic Acid	4	6299	-6.402	-7.881		-21.626	-21.641
9/13/2016	Aspartic Acid	4	8237	-3.244	-7.501		10.569	10.855
9/19/2016	Aspartic Acid	3	8626	-4.021	-7.114		10.725	11.067
9/20/2016	Aspartic Acid	3	8689	-4.051	-7.198		10.691	11.075
2/1/2017	Aspartic Acid	4	4839	-2.784	-6.241	10936		10.633
4/27/2017	Aspartic Acid	3	6741	-4.225	-7.077	6205	10.689	10.489
3/5/2018	Aspartic Acid			-3.658	-7.299		10.858	10.485
3/7/2018	Aspartic Acid	4	4393	-2.712	-5.825	4717	10.906	10.837
3/7/2018	Aspartic Acid	6	1135	-3.596	-6.693	4902	-21.363	-21.512
3/13/2018	Aspartic Acid	4	4219	-1.979	-6.485	4241	10.920	10.698
4/12/2018	Aspartic Acid	4	4331	-5.322	-7.391	4303	10.606	10.591
5/9/2018	Aspartic Acid	5	4173	-3.161	-6.841	4284	10.802	10.482
5/10/2018	Aspartic Acid	6	4343	-2.746		4558	10.657	9.770
5/10/2018	Aspartic Acid	3	4727	-2.869		4919	10.608	9.722
10/3/2018	Aspartic Acid	4	5602	-3.534	-7.266	5369	10.834	10.575
10/4/2018	Aspartic Acid	4	6220	-3.205		5846	10.790	10.367
10/11/2018	Aspartic Acid	4	4763	-2.476	-7.467	4459	10.872	9.862
11/1/2018	Aspartic Acid	4	4827	-4.971	-6.541	4526	10.719	10.093
11/1/2018	Aspartic Acid	7	1138	-5.021	-6.590	4365	-21.733	-22.220
11/2/2018	Aspartic Acid	4	4170	-4.127	-7.038	3916	10.726	10.157
11/20/2018	Aspartic Acid	4	4845	-5.081	-7.141	4427	10.732	9.974
11/29/2018	Aspartic Acid	4	5510	-3.889	-7.466	5045	10.745	10.052
3/6/2019	Aspartic Acid	7	5146	-6.185	-7.110	4709	-21.143	-21.816
3/6/2019	Aspartic Acid	4	5813	-5.804	-6.728	5175	11.075	10.889
3/6/2019	Aspartic Acid	32	4695	-6.537	-7.463	4510	10.820	10.630
3/8/2019	Aspartic Acid	4	5190	-6.628	-8.234	4482	11.095	10.398
3/22/2019	Aspartic Acid	4	4711	-7.473	-7.487	4709	10.517	10.263
3/25/2019	Aspartic Acid	4	5950	-7.528		5949	10.865	9.960
3/25/2019	Aspartic Acid	28	5857	-7.163		5874	10.602	9.699
3/28/2019	Aspartic Acid	4	5217	-6.475		5060	10.568	9.807
4/2/2019	Aspartic Acid	80	6733	-6.242		6582	-21.286	-21.973
4/2/2019	Aspartic Acid	4	7022	-6.372		6637	10.853	10.163
4/6/2019	Aspartic Acid	69	5976	-3.600		20220	-24.936	-25.005
4/6/2019	Aspartic Acid	4	5279	-6.547		5227	10.695	10.493
4/11/2019	Aspartic Acid	3	5614	-5.567		5557	10.645	9.868
4/11/2019	Aspartic Acid	6	7547	-6.023		7275	10.899	10.450
4/30/2019	Aspartic Acid	4	4407	-5.503		4413	10.691	9.594
4/30/2019	Aspartic Acid	4	4407	-5.503		4413	10.691	9.594
8/6/2019	Aspartic Acid	48				5423	-21.556	-22.039
8/6/2019	Aspartic Acid	48				5423	-21.556	-22.039
8/6/2019	Aspartic Acid	4				11976	-20.966	-21.446
8/6/2019	Aspartic Acid	45				4889	10.633	10.333
8/6/2019	Aspartic Acid	4				11976	-20.966	-21.446
8/6/2019	Aspartic Acid	45				4889	10.633	10.333
8/13/2019	Aspartic Acid	7				4274	-21.404	-21.901
8/13/2019	Aspartic Acid	7				4274	-21.404	-21.901
10/29/2019	Aspartic Acid	4	7040	-5.755	-6.17082	5832	11.181	10.567
10/29/2019	Aspartic Acid	47	5024	-7.378	-7.79236	4473	10.773	10.977
10/30/2019	Aspartic Acid	3	5559	-7.605	-7.63887	4898	10.742	10.154
10/30/2019	Aspartic Acid	46	6287	-7.442	-7.46031	5479	10.684	10.097
11/12/2019	Aspartic Acid	7	6996	-7.864	-7.74762	18137	-20.793	-21.276
11/12/2019	Aspartic Acid	4	3907	-8.106	-7.99296	3658	-21.478	-21.956
1/30/2020	Aspartic Acid	5	7419	-7.634		7749	11.150	10.352
1/30/2020	Aspartic Acid	47	7376	-6.170	-6.44478	7928	11.101	10.303
2/4/2020	Aspartic Acid	6	5067	-5.161	-6.36698	5655	10.763	9.685
2/4/2020	Aspartic Acid	8	6274	-5.496	-6.70319	6934	-21.296	-21.999
2/4/2020	Aspartic Acid	37	3911	-3.592	-5.31525	4603	10.926	9.846
2/14/2020	Aspartic Acid	49	6880	-5.668	-6.54296	7960	-21.257	-21.706
2/14/2020	Aspartic Acid	5	5725	-6.272	-6.99637	6473	10.851	10.325
2/21/2020	Aspartic Acid	5	7600	-6.165	-6.969	8490	11.060	10.432
3/28/2020	Aspartic Acid	4	5217	-6.475		5060	10.568	9.807
4/2/2020	Aspartic Acid	80	6733	-6.242		6582	-21.286	-21.973
4/2/2020	Aspartic Acid	4	7022	-6.372		6637	10.853	10.163
4/6/2020	Aspartic Acid	69	5976	-3.600		20220	-24.936	-25.005
4/6/2020	Aspartic Acid	4	5279	-6.547		5227	10.695	10.493
4/7/2020	Aspartic Acid	5	6869	-5.932	-6.73	7721	11.150	10.288
4/7/2020	Aspartic Acid	39	8011	-6.130	-6.934	8952	11.229	10.366

4/24/2014 CH 3	5	5315	-23.416	-24.724	-24.488
4/16/2015 CH 3	41	4975	-24.801	-24.724	-24.692
5/6/2015 CH 3	26	6075	-24.700	-24.724	-24.606
5/6/2015 CH 3	32	6911	-24.672	-24.724	-24.578
10/16/2015 CH 3	7		-24.607		-24.632
9/13/2016 CH 3	8		-25.090	-24.724	-24.605
9/19/2016 CH 3	7		-25.105	-24.724	-24.619
9/20/2016 CH 3	7		-25.196	-24.724	-24.683
9/21/2016 CH 3	7		-25.100	-24.724	-24.608
9/21/2016 CH 3	28		-25.055	-24.724	-24.563
11/23/2016 CH 3	6		-24.522	-24.724	-24.637
2/1/2017 CH 3	9				-24.662
4/27/2017 CH 3	7	7210	-24.462	-24.724	-24.613
3/5/2018 CH 3			-24.488	-24.724	-24.670
3/7/2018 CH 3	8	4638	-24.442	-24.724	-24.599
3/7/2018 CH 3	62	4958	-25.047	-24.724	-25.206
3/13/2018 CH 3	9	4829	-24.429	-24.724	-24.609
4/12/2018 CH 3	9	5032	-24.435	-24.724	-24.692
5/10/2018 CH 3	8	29632	-22.794	-24.724	-24.725
10/3/2018 CH 3	9	5234	-24.512	-24.724	-24.689
10/4/2018 CH 3	8	10259	-24.249	-24.724	-24.775
10/11/2018 CH 3	9	9911	-24.233	-24.724	-24.586
10/11/2018 CH 3	72	10781	-24.192	-24.724	-24.546
11/1/2018 CH 3	9	10929	-24.218	-24.724	-24.694
11/1/2018 CH 3	50	9996	-24.326	-24.724	-24.802
11/2/2018 CH 3	8	11597	-24.192	-24.724	-24.649
11/20/2018 CH 3	9	11970	-24.179	-24.724	-24.598
11/20/2018 CH 3	52	11466	-24.255	-24.724	-24.673
11/29/2018 CH 3	11	9648	-24.385	-24.724	-24.663
11/30/2018 CH 3	11	11409	-24.295	-24.724	-24.520
11/30/2018 CH 3	52	11593	-24.221	-24.724	-24.699
3/6/2019 CH 3	8	11138	-23.908	-24.724	-24.623
3/6/2019 CH 3	36	12735	-24.108	-24.724	-24.826
3/8/2019 CH 3	8	10776	-23.987	-24.724	-24.761
3/22/2019 CH 3	9	11023	-24.137	-24.724	-24.460
3/22/2019 CH 3	44	13557	-23.938	-24.724	-24.261
3/22/2019 CH 3	83	4727	-24.639	-24.724	-24.969
3/25/2019 CH 3	9	11636	-24.059	-24.724	-24.678
3/25/2019 CH 3	33	11277	-24.062	-24.724	-24.681
3/28/2019 CH 3	9	13796	-23.713	-24.724	-24.419
3/28/2019 CH 3	54	9701	-23.968	-24.724	-24.674
4/2/2019 CH 3	9	11600	-24.47	-24.724	-25.072
4/2/2019 CH 3	43	11368	-23.821	-24.724	-24.425
4/2/2019 CH 3	83	11317	-23.773	-24.724	-24.449
4/6/2019 CH 3	9	9925	-23.987	-24.724	-24.432
4/6/2019 CH 3	42	10484	-24.469	-24.724	-24.917
4/6/2019 CH 3	72	11954	-25.133	-24.724	-25.208
4/11/2019 CH 3	15	9267	-24.075	-24.724	-24.724
4/11/2019 CH 3	11	10982	-23.854	-24.724	-24.724
4/30/2019 CH 3	9	9932	-23.873	-24.724	-24.513
4/30/2019 CH 3	45	10204	-23.91	-24.724	-24.550
4/30/2019 CH 3	9	9932	-23.873	-24.724	-24.513
4/30/2019 CH 3	45	10204	-23.91	-24.724	-24.550
8/6/2019 CH 3	9	10451	-24.139	-24.724	-24.637
8/6/2019 CH 3	43	8993	-24.279	-24.724	-24.778
8/6/2019 CH 3	9	10451	-24.139	-24.724	-24.637
8/6/2019 CH 3	43	8993	-24.279	-24.724	-24.778
8/6/2019 CH 3	76	9591	-24.255	-24.724	-24.754
8/13/2019 CH 3	9	8090	-24.102	-24.724	-24.585
8/13/2019 CH 3	45	9433	-24.07	-24.724	-24.699
8/13/2019 CH 3	9	8090	-24.102	-24.724	-24.585
10/29/2019 CH 3	7	9137	-23.844	-24.724	-24.679
10/29/2019 CH 3	50	10835	-23.929	-24.724	-24.683
10/30/2019 CH 3	6	9894	-24.187	-24.724	-24.611
10/30/2019 CH 3	49	9504	-24.218	-24.724	-24.641
11/12/2019 CH 3	8	9211	-24.308	-24.724	-24.769
1/30/2020 CH 3	9	12032	-23.937	-24.724	-24.591
1/30/2020 CH 3	50	12465	-23.995	-24.724	-24.649
1/30/2020 CH 3	86	12195	-24.062	-24.724	-24.716
2/4/2020 CH 3	9	10817	-24.016	-24.724	-24.687
2/4/2020 CH 3	40	13406	-23.871	-24.724	-24.544
2/4/2020 CH 3	70	12717	-24.02	-24.724	-24.691
2/14/2020 CH 3	8	11397	-24.198	-24.724	-24.640
2/14/2020 CH 3	51	10294	-24.207	-24.724	-24.649
2/21/2020 CH 3	8	11316	-24.144	-24.724	-24.673
2/21/2020 CH 3	50	14123	-23.93	-24.724	-24.460
2/21/2020 CH 3	86	11520	-24.098	-24.724	-24.627
3/28/2020 CH 3	9	13796	-23.713	-24.724	-24.419
3/28/2020 CH 3	54	9701	-23.968	-24.724	-24.674
4/2/2020 CH 3	9	11600	-24.47	-24.724	-25.072
4/2/2020 CH 3	83	11317	-23.773	-24.724	-24.449
4/6/2020 CH 3	9	9925	-23.987	-24.724	-24.432
4/6/2020 CH 3	42	10484	-24.469	-24.724	-24.917
4/6/2020 CH 3	72	11954	-25.133	-24.724	-25.208
4/7/2020 CH 3	8	10348	-24.137	-24.724	-24.749
4/7/2020 CH 3	68	11726	-24.007	-24.724	-24.620

1/30/2014 CH 6	5	5868	-10.914	-10.449	-10.331
4/24/2014 CH 6	4	30504	-9.353	-10.449	-10.599
4/16/2015 CH 6	40	6397	-10.567		-10.493
5/6/2015 CH 6	25	6767	-10.539	-10.449	-10.449
5/6/2015 CH 6	33	6251	-10.632	-10.449	-10.542
10/8/2015 CH 6	9		-10.231		-10.307
10/16/2015 CH 6	8		-10.673		-10.652
9/13/2016 CH 6	9		-10.996	-10.449	-10.590
9/19/2016 CH 6	8		-10.965	-10.449	-10.536
9/20/2016 CH 6	8		-11.015	-10.449	-10.553
9/21/2016 CH 6	8		-10.995	-10.449	-10.542
9/21/2016 CH 6	29		-10.984	-10.449	-10.531
11/23/2016 CH 6	7		-10.347	-10.449	-10.474
2/1/2017 CH 6	10				-10.447
4/27/2017 CH 6	8	6680	-10.362	-10.449	-10.533
3/5/2018 CH 6			-10.230	-10.449	-10.489
3/7/2018 CH 6	9	5909	-10.160	-10.449	-10.281
3/7/2018 CH 6	63	4670	-10.278	-10.449	-10.400
3/13/2018 CH 6	10	5200	-10.487	-10.449	-10.683
4/12/2018 CH 6	10	5828	-10.273	-10.449	-10.432
5/9/2018 CH 6	11	6316	-10.292	-10.449	-10.631
5/10/2018 CH 6	9	7754	-10.623	-10.449	-10.449
10/3/2018 CH 6	10	5011	-10.394	-10.449	-10.458
10/4/2018 CH 6	9	11128	-9.995	-10.449	-10.538
10/11/2018 CH 6	10	13863	-9.783	-10.449	-10.407
10/11/2018 CH 6	73	16686	-9.652	-10.449	-10.278
11/1/2018 CH 6	10	13294	-9.936	-10.449	-10.473
11/1/2018 CH 6	51	14048	-9.813	-10.449	-10.351
11/2/2018 CH 6	9	12756	-9.961	-10.449	-10.463
11/20/2018 CH 6	10	13947	-9.908	-10.449	-10.465
11/20/2018 CH 6	53	12195	-9.995	-10.449	-10.552
11/29/2018 CH 6	12	10859	-10.182	-10.449	-10.628
11/30/2018 CH 6	12	9447	-10.295	-10.449	-10.689
11/30/2018 CH 6	53	11987	-10.109	-10.449	-10.341
3/6/2019 CH 6	9	10760	-9.896	-10.449	-10.399
3/6/2019 CH 6	37	11737	-9.997	-10.449	-10.502
3/8/2019 CH 6	9	10794	-9.782	-10.449	-10.525
3/22/2019 CH 6	10	10147	-10.130	-10.449	-10.425
3/22/2019 CH 6	45	10588	-10.052	-10.449	-10.347
3/22/2019 CH 6	84	3782	-10.600	-10.449	-10.696
3/25/2019 CH 6	10	11930	-9.864	-10.449	-10.599
3/25/2019 CH 6	34	12934	-9.762	-10.449	-10.498
3/28/2019 CH 6	10	10009	-9.820	-10.449	-10.549
3/28/2019 CH 6	55	9398	-9.844	-10.449	-10.573
4/2/2019 CH 6	10	10508	-9.740	-10.449	-10.379
4/2/2019 CH 6	44	9280	-9.854	-10.449	-10.593
4/2/2019 CH 6	84	14860	-9.367	-10.449	-10.108
4/6/2019 CH 6	10	8774	-10.024	-10.449	-10.371
4/6/2019 CH 6	43	11781	-10.248	-10.449	-9.838
4/6/2019 CH 6	73	13810	-11.287	-10.449	-10.911
4/11/2019 CH 6	16	11784	-9.747	-10.449	-10.449
4/11/2019 CH 6	12	10871	-9.724	-10.449	-10.423
4/11/2019 CH 6	34	10133	-9.776	-10.449	-10.475
4/30/2019 CH 6	10	9102	-9.828	-10.449	-10.654
4/30/2019 CH 6	46	11730	-9.662	-10.449	-10.490
4/30/2019 CH 6	10	9102	-9.828	-10.449	-10.654
4/30/2019 CH 6	46	11730	-9.662	-10.449	-10.490
8/6/2019 CH 6	75	9793	-10.035	-10.449	-10.453
8/6/2019 CH 6	10	9770	-10.032	-10.449	-10.450
8/6/2019 CH 6	44	10216	-10.027	-10.449	-10.445
8/6/2019 CH 6	10	9770	-10.032	-10.449	-10.450
8/6/2019 CH 6	44	10216	-10.027	-10.449	-10.445
8/13/2019 CH 6	10	8463	-9.979	-10.449	-10.538
8/13/2019 CH 6	46	2961	-10.629	-10.449	-10.793
8/13/2019 CH 6	10	8463	-9.979	-10.449	-10.538
10/29/2019 CH 6	8	10817	-9.509	-10.449	-10.253
10/29/2019 CH 6	51	9936	-9.904	-10.449	-10.271
10/30/2019 CH 6	7	10880	-9.872	-10.449	-10.363
10/30/2019 CH 6	50	9612	-10.067	-10.449	-10.557
11/12/2019 CH 6	9	11896	-9.957	-10.449	-10.507
1/30/2020 CH 6	10	12099	-9.771	-10.449	-10.483
1/30/2020 CH 6	51	11396	-9.938	-10.449	-10.650
1/30/2020 CH 6	87	13041	-9.824	-10.449	-10.536
2/4/2020 CH 6	10	13141	-9.778	-10.449	-10.615
2/4/2020 CH 6	41	16129	-9.507	-10.449	-10.348
2/4/2020 CH 6	71	15219	-9.706	-10.449	-10.544
2/14/2020 CH 6	9	13791	-10.001	-10.449	-10.477
2/14/2020 CH 6	52	12617	-9.916	-10.449	-10.392
2/21/2020 CH 6	9	12650	-9.892	-10.449	-10.461
2/21/2020 CH 6	51	13628	-9.765	-10.449	-10.334
2/21/2020 CH 6	87	11591	-9.968	-10.449	-10.537
3/28/2020 CH 6	10	10009	-9.820	-10.449	-10.549
3/28/2020 CH 6	55	9398	-9.844	-10.449	-10.573
4/2/2020 CH 6	10	10508	-9.740	-10.449	-10.379
4/2/2020 CH 6	84	14860	-9.367	-10.449	-10.108
4/6/2020 CH 6	10	8774	-10.024	-10.449	-10.371
4/6/2020 CH 6	43	11781	-10.248	-10.449	-9.838
4/6/2020 CH 6	73	13810	-11.287	-10.449	-10.911
4/7/2020 CH 6	9	10766	-9.934	-10.449	-10.647
4/7/2020 CH 6	69	16965	-9.588	-10.449	-10.303

5/6/2015	Nicotinamide	4				9057	-34.345	-34.248
5/6/2015	Nicotinamide	5				9680	-34.316	-34.219
5/6/2015	Nicotinamide	8				7706	-34.437	-34.340
10/8/2015	Nicotinamide	6					-34.192	-34.143
10/8/2015	Nicotinamide	4					-34.252	-34.203
10/16/2015	Nicotinamide	3	15773	1.125	-0.262		-34.164	-34.221
9/13/2016	Nicotinamide	5	14740	4.046	-0.058		-34.787	-34.247
9/19/2016	Nicotinamide	4	18926	3.091	-0.042		-34.688	-34.164
9/20/2016	Nicotinamide	4	18729	2.878	-0.310		-34.702	-34.155
9/21/2016	Nicotinamide	4	12746	3.37	-0.041		-34.875	-34.355
11/23/2016	Nicotinamide	2	14896	2.797			-34.164	-34.270
11/23/2016	Nicotinamide	3	14750	2.948			-34.214	-34.320
2/1/2017	Nicotinamide	5	14256	3.403	-0.007	8961	-34.296	-34.359
2/1/2017	Nicotinamide	7	14191	3.561	0.152	5550	-24.520	-34.450
4/27/2017	Nicotinamide	4	17543	2.581	-0.283	11327	-34.121	-34.258
4/27/2017	Nicotinamide	5	17309	2.616	-0.248	11171	-34.123	-34.260
3/5/2018	Nicotinamide			3.135	-0.564		-34.022	-34.153
3/5/2018	Nicotinamide			3.196	-0.504		-34.102	-34.232
3/7/2018	Nicotinamide	3	8776	3.995	0.760	6775	-34.124	-34.305
3/7/2018	Nicotinamide	5	8234	3.817	0.586	6313	-34.123	-34.304
3/13/2018	Nicotinamide	3	10122	3.963	-0.558	7081	-34.079	-34.247
3/13/2018	Nicotinamide	5	10141	3.959	-0.562	7084	-34.097	-34.265
4/12/2018	Nicotinamide	5	10943	1.963	-0.103	7597	-33.986	-34.309
4/12/2018	Nicotinamide	7	13718	1.994	-0.072	9398	-33.914	-34.237
5/9/2018	Nicotinamide	6	10819	3.208	-0.355	7607	-34.001	-34.361
5/10/2018	Nicotinamide	4	10121	3.599		7407	-34.044	-34.573
10/3/2018	Nicotinamide	5	12800	3.306	-0.445	8595	-33.947	-33.964
10/3/2018	Nicotinamide	6	12986	3.279	-0.472	8679	-33.937	-33.955
10/11/2018	Nicotinamide	5	8148	4.21	-0.626	5519	-34.070	-34.239
11/1/2018	Nicotinamide	5	8142	1.814	0.125	5521	-34.258	-34.691
11/2/2018	Nicotinamide	5	9605	2.426	-0.594	6478	-34.196	-34.621
11/2/2018	Nicotinamide	7	7819	2.522	-0.500	5326	-34.325	-34.749
11/20/2018	Nicotinamide	5	14528	2.152	0.089	9359	-33.998	-34.322
11/20/2018	Nicotinamide	7	12583	2.113	0.050	8214	-34.081	-34.404
11/29/2018	Nicotinamide	5	11962	2.926	-0.585	7737	-34.102	-34.265
11/29/2018	Nicotinamide	7	15736	2.894	-0.617	10156	-34.157	-34.320
11/30/2018	Nicotinamide	5	14016	2.938	-0.625	9025	-34.013	-34.120
11/30/2018	Nicotinamide	7	11921	2.98	-0.583	7774	-34.274	-34.378
3/6/2019	Nicotinamide	5	12768	1.114	0.214	8363	-33.750	-34.613
3/6/2019	Nicotinamide	33	13678	0.803	-0.098	9228	-34.001	-34.868
3/6/2019	Nicotinamide	35	11032	0.862	-0.039	7605	-34.145	-35.014
3/8/2019	Nicotinamide	7	11383	1.012	-0.530	6993	-33.945	-34.741
3/8/2019	Nicotinamide	32	11424	1.23	-0.310	7125	-33.997	-34.793
3/22/2019	Nicotinamide	5	13400	-0.207	-0.145	9436	-33.978	-34.321
3/22/2019	Nicotinamide	7	11277	-0.191	-0.129	8010	-34.115	-34.458
3/25/2019	Nicotinamide	5	13391	-0.292		9523	-33.946	-34.484
3/25/2019	Nicotinamide	7	11680	-0.26		8393	-34.013	-34.550
3/25/2019	Nicotinamide	29	12301	0.142		8811	-34.046	-34.583
3/25/2019	Nicotinamide	31	14610	0.068		10265	-33.866	-34.404
3/28/2019	Nicotinamide	5	12895	0.627		8623	-33.835	-34.525
3/28/2019	Nicotinamide	7	13173	0.551		8806	-33.816	-34.506
4/2/2019	Nicotinamide	5	13943	0.528		9412	-33.727	-34.306
4/2/2019	Nicotinamide	7	12826	0.552		8716	-33.831	-34.410
4/2/2019	Nicotinamide	41	15975	0.561		10628	-33.689	-34.268
4/6/2019	Nicotinamide	5	14907	0.752		10040	-33.947	-34.461
4/6/2019	Nicotinamide	7	13214	0.814		9029	-33.834	-34.347
4/11/2019	Nicotinamide	4	8522	1.267		6166	-34.046	-34.658
4/11/2019	Nicotinamide	5	12375	0.955		8598	-33.889	-34.880
4/30/2019	Nicotinamide	5	9981	1.235		7154	-33.907	-34.415
4/30/2019	Nicotinamide	7	12885	0.99		9029	-33.829	-34.338
4/30/2019	Nicotinamide	43	10076	1.362		7257	-34.017	-34.523
4/30/2019	Nicotinamide	5	9981	1.235		7154	-33.907	-34.415
4/30/2019	Nicotinamide	7	12885	0.99		9029	-33.829	-34.338
4/30/2019	Nicotinamide	43	10076	1.362		7257	-34.017	-34.523
8/6/2019	Nicotinamide	5				6532	-34.069	-34.624
8/6/2019	Nicotinamide	46				8209	-33.976	-34.530
8/6/2019	Nicotinamide	5				6532	-34.069	-34.624
8/6/2019	Nicotinamide	46				8209	-33.976	-34.530
8/13/2019	Nicotinamide	5				6214	-33.966	-34.396
8/13/2019	Nicotinamide	5				6214	-33.966	-34.396
10/29/2019	Nicotinamide	5	11331	0.729	0.307	6944	-33.705	-34.602
10/29/2019	Nicotinamide	48	13250	-0.036	-0.457	8234	-33.859	-34.887
10/30/2019	Nicotinamide	4	10937	-0.332	-0.292	6914	-34.22	-34.596
10/30/2019	Nicotinamide	47	11534	-0.274	-0.226	7289	-34.091	-34.468
11/12/2019	Nicotinamide	5	13158	-0.417	-0.198	8402	-34.115	-34.515
1/30/2020	Nicotinamide	6	13381	-0.458	-0.623	10254	-33.942	-34.555
1/30/2020	Nicotinamide	48	13502	0.565	0.420	10383	-33.906	-34.519
2/4/2020	Nicotinamide	7	13034	0.966	-0.218	10260	-33.902	-34.457
2/4/2020	Nicotinamide	38	12029	1.146	-0.538	9526	-33.935	-34.490
2/14/2020	Nicotinamide	6	13386	0.422	-0.219	10783	-33.995	-34.414
2/14/2020	Nicotinamide	50	16210	0.518	-0.246	12976	-33.853	-34.272
2/21/2020	Nicotinamide	6	12942	0.668	-0.052	10463	-33.931	-34.433
2/21/2020	Nicotinamide	49	14745	0.674	-0.046	11797	-33.83	-34.332
3/28/2020	Nicotinamide	5	12895	0.627		8623	-33.835	-34.525
3/28/2020	Nicotinamide	7	13173	0.551		8806	-33.816	-34.506
4/2/2020	Nicotinamide	5	13943	0.528		9412	-33.727	-34.306
4/2/2020	Nicotinamide	7	12826	0.552		8716	-33.831	-34.410
4/6/2020	Nicotinamide	5	14907	0.752		10040	-33.947	-34.461
4/6/2020	Nicotinamide	7	13214	0.814		9029	-33.834	-34.347
4/7/2020	Nicotinamide	6	13240	0.733	-0.014	10661	-33.893	-34.435
4/7/2020	Nicotinamide	40	14183	0.687	-0.060	11438	-33.925	-34.467

Non-exclusive licence to reproduce thesis and make thesis public

I**, MARGARITA ESMERALDA GONZALES FERRAZ,**

1. herewith grant the University of Tartu a free permit (non-exclusive licence) to reproduce, for the purpose of preservation, including for adding to the DSpace digital archives until the expiry of the term of copyright,

ISOTOPIC STABILITY OF MASS REFERENCE MATERIALS AND POSSIBLE USE AS ISOTOPIC REFERENCE MATERIALS,

supervised by Professor KALLE KIRSIMÄE, HOLAR SEPP.

2. I grant the University of Tartu a permit to make the work specified in p. 1 available to the public via the web environment of the University of Tartu, including via the DSpace digital archives, under the Creative Commons licence CC BY NC ND 3.0, which allows, by giving appropriate credit to the author, to reproduce, distribute the work and communicate it to the public, and prohibits the creation of derivative works and any commercial use of the work until the expiry of the term of copyright.

3. I am aware of the fact that the author retains the rights specified in p. 1 and 2.

4. I certify that granting the non-exclusive licence does not infringe other persons intellectual property rights or rights arising from the personal data protection legislation.

author's name: Margarita Esmeralda Gonzales Ferraz

20/08/2020